ผลของปริมาณธาตุโมลิบดีนัมต่อพฤติกรรมกรรมวิธีทางความร้อนของเหล็กหล่อขาว
ธาตุผสมหลายธาตุ

นายธนิศร์ มีบุปผา

วิทยานิพนธ์นี้เป็นส่วนหนึ่งของการศึกษาตามหลักสูตรปริญญาวิศวกรรมศาสตรมหาบัณฑิต
สาขาวิชาวิศวกรรมโลหการและวัสดุ ภาควิชาวิศวกรรมโลหการ
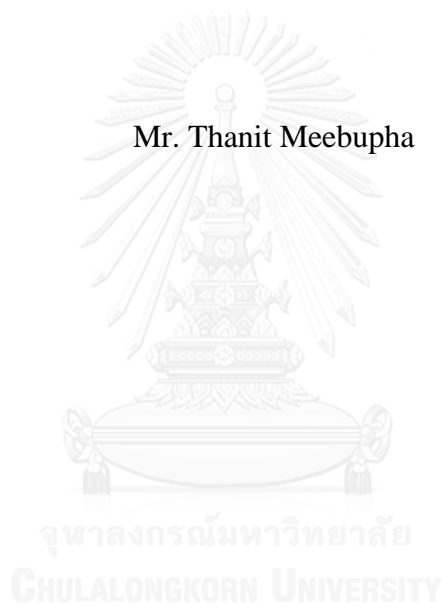คณะวิศวกรรมศาสตร์ จุฬาลงกรณ์มหาวิทยาลัย
ปีการศึกษา 2558

EFFECT OF MOLYBDENUM CONTENT ON HEAT TREATMENT BEHAVIOR
OF MULTI-ALLOYED WHITE CAST IRON

Mr. Thanit Meebupha

Thesis Title	EFFECT OF MOLYBDENUM CONTENT ON HEAT TREATMENT BEHAVIOR OF MULTI-ALLOYED WHITE CAST IRON
By	Mr. Thanit Meebupha
Field of Study	Metallurgical and Materials Engineering
Thesis Advisor	Associate ProfessorPrasonk Sricharoenchai, D.Eng.
Thesis Co-Advisor	ProfessorYasuhiro Matsubara, D.Eng.

Accepted by the Faculty of Engineering, Chulalongkorn University in Partial Fulfillment of the Requirements for the Master's Degree

....Dean of the Faculty of Engineering
(Associate ProfessorSupot Teachavorasinskun, D.Eng.)

THESIS COMMITTEE

....Chairman
(Assistant ProfessorMawin Supradist na ayudhaya, D.Eng.)
....Thesis Advisor
(Associate ProfessorPrasonk Sricharoenchai, D.Eng.)
....Thesis Co-Advisor
(ProfessorYasuhiro Matsubara, D.Eng.)
....Examiner
(Associate ProfessorCharkorn Jarupisitthorn, M.Eng.)
....External Examiner
(Associate ProfessorSudsakorn Inthidech, D.Eng.)

ธนิศร์ มีบุปผา : ผลของปริมาณธาตุโมลิบดีนัมต่อพฤติกรรมกรรมวิธีทางความร้อนของเหล็กหล่อขาว
ธาตุผสมหลายธาตุ (EFFECT OF MOLYBDENUM CONTENT ON HEAT TREATMENT
BEHAVIOR OF MULTI-ALLOYED WHITE CAST IRON) อ.ที่ปรึกษาวิทยานิพนธ์หลัก: รศ.
ดร.ประสงค์ ศรีเจริญชัย, อ.ที่ปรึกษาวิทยานิพนธ์ร่วม: ศ. ดร.ยาสุฮิโระ มัตสึบาระ, 116 หน้า.

เหล็กหล่อขาวธาตุผสมหลายธาตุ ประกอบด้วยธาตุผสมซึ่งเกิดคาร์ไบด์ได้ กล่าวคือ วาเนเดียม
โครเมียม โมลิบดีนัม และ ทังสเตน เพื่อให้เกิดคาร์ไบด์ชนิดต่างๆระหว่างการแข็งตัว ในธาตุผสมเหล่านี้
โมลิบดีนัมเป็นธาตุที่มีประโยชน์มากธาตุหนึ่ง ซึ่งไม่เพียงแต่เกิดยูเทกติกคาร์ไบด์ แต่ยังละลายในเนื้อพื้นเพื่อ
ปรับปรุงคุณลักษณะพิเศษของกรรมวิธีทางความร้อน เพื่อตรวจสอบผลของปริมาณโมลิบดีนัมต่อพฤติกรรม
กรรมวิธีทางความร้อนของเหล็กหล่อขาวธาตุผสมหลายธาตุ ได้เตรียมชิ้นงานทดสอบที่แปรผันปริมาณโมลิบดีนัม
ตั้งแต่ 0 ถึง 7.66% โดยมวล หลังการอบอ่อน ได้อบชิ้นงานทดสอบในเตาสุญญากาศที่อุณหภูมิ 1,373 เคลวิน
เป็นเวลา 3,600 วินาที และชุบแข็งด้วยไนโตรเจนเหลว อบคืนตัวชิ้นงานที่ชุบแข็งแล้วที่อุณหภูมิต่างๆ ระหว่าง
673 เคลวิน ถึง 873 เคลวิน เป็นเวลา 12,000 วินาที

เมื่อปริมาณโมลิบดีนัมของชิ้นงานเพิ่มขึ้น ความแข็งมาโครและความแข็งไมโครในสภาพชุบแข็ง
เพิ่มขึ้นอย่างต่อเนื่อง ในสภาพอบคืนตัวเส้นโค้งความแข็งแสดงการแข็งขึ้นทุติยภูมิ กล่าวคือ ความแข็งเพิ่มขึ้น
ก่อนถึงค่าสูงสุดและลดลงตามการเพิ่มขึ้นของอุณหภูมิอบคืนตัว เหตุผลของการเกิดการแข็งขึ้นทุติยภูมิ คือ การ
ตกตะกอนของคาร์ไบด์พิเศษ จากมาร์เทนไซต์โดยปฏิกิริยาคาร์ไบด์ และการแปลงเฟสเป็นมาร์เทนไซต์ จาก
ออสเทไนต์ที่เหลืออยู่ระหว่างการเย็นตัวต่อมา ความแข็งสูงสุดหลังอบคืนตัว (H_{Tmax}) พบในชิ้นงานที่อบคืนตัวที่
อุณหภูมิ 798 เคลวิน ในทุกปริมาณโมลิบดีนัม และค่าสูงสุดของ H_{Tmax} คือ 946 HV30 ในชิ้นงานที่มีโมลิบดีนัม
4.98% โดยมวล

สัดส่วนเชิงปริมาตรของออสเทไนต์เหลือค้าง (V_γ) ในสภาพชุบแข็ง ลดลงอย่างช้าๆ ตามการเพิ่มขึ้น
ของปริมาณโมลิบดีนัม ในสภาพอบคืนตัว V_γ เริ่มลดลงอย่างชัดเจนเมื่ออุณหภูมิอบคืนตัวสูงกว่า 748 เคลวิน ใน
ทุกชิ้นงาน V_γ ที่ค่าความแข็งสูงสุดหลังอบคืนตัวมีค่าน้อยกว่า 10% โดยปริมาตร และ V_γ ที่ค่าความแข็งสูงสุด
หลังอบคืนตัวลดลงเป็นสัดส่วนกันจาก 10% ถึง 2% เมื่อปริมาณโมลิบดีนัมเพิ่มขึ้น

5770195221 : MAJOR METALLURGICAL AND MATERIALS ENGINEERING

KEYWORDS: MULTI-ALLOTED WHITE CAST IRON, HEAT-TREATMENT, HARDNESS, VOLUME FRACTION OF RETAINED AUSTENITE, MO EFFECT

THANIT MEEBUPHA: EFFECT OF MOLYBDENUM CONTENT ON HEAT TREATMENT BEHAVIOR OF MULTI-ALLOYED WHITE CAST IRON. ADVISOR: ASSOC. PROF.PRASONK SRICHAROENCHAI, D.Eng., CO-ADVISOR: PROF.YASUHIRO MATSUBARA, D.Eng., 116 pp.

Multi-alloyed white cast iron contains several kinds of carbide forming elements namely V, Cr, Mo and W to form their own carbides during solidification. In such alloying elements, Mo is very useful one which not only forms eutectic carbide but also dissolves into matrix to improve the characteristics of heat treatment. In order to investigate the effect of Mo content on the heat treatment behavior, the multi-alloyed white cast iron varying Mo content from nil to 7.66 mass% were prepared. After annealing, test pieces in disk shape were austenitized at 1,373K for 3.6 ks in vacuum furnace and then, hardened by liquid nitrogen. The hardened specimens were tempered at various temperatures between 673 and 873K for 12 ks.

As Mo content of the specimen increased, the macro- and micro-hardness in as-hardened state increased progressively. In tempered state, hardness curves showed secondary hardening, i.e. with increasing of tempering temperature; the hardness rose first to the maximum value and then decreased. The reason why secondary hardening takes place is mainly due to the precipitation of special carbides from martensite by carbide reaction and the martensite transformation from the rest of austenite during post cooling. The maximum tempered hardness (H_{Tmax}) was obtained at 798K tempering, regardless of Mo content of specimens and the highest H_{Tmax} was 946 HV30 in specimen with 4.98%Mo.

Volume fraction of retained austenite (V_γ) in as-hardened state decreases gradually with an increase in Mo content. In tempered state, the V_γ began to decrease remarkably as the tempering temperature got over 748K in all the specimens. The V_γ values at H_{Tmax} were less than 10% and the V_γ at H_{Tmax} decreased proportionally from 10% to 2% as the Mo content is increased.

Department: Metallurgical Engineering   Student's Signature ------------------------------

Field of Study: Metallurgical and Materials   Advisor's Signature ------------------------------

       Engineering   Co-Advisor's Signature ------------------------------

Academic Year: 2015

ACKNOWLEDGEMENTS

CONTENTS

LIST OF TABLES

LIST OF FIGURES

Chapter I

Introduction

1.1 Background

In the industries of steel-making, mining, cement and thermal power plant, many types of machines are used for crushing, mixing or pulverizing of ores and their products. The severe abrasive wear takes place frequently in the parts or components of such machines. The alloyed white cast irons have been adopted for such parts and components because of higher wear resistance compared with steels that have high toughness but low wear resistance.

In the field of the steel industry, the materials for rolling mill rolls have been developed to improve the quality of products and their productivity. The research and development have been focused on the improvement of work rolls to achieve an economical operation. The main purpose is to improve the mechanical properties like hardness, toughness and wear resistance. This work led the rolls to increase not only their service life but also the productivity. As examples of typical abrasion wear resistant materials, the evolution of cast iron materials for last half century is shown in Fig. 1-1.

The chilled cast iron was replaced by indefinite chilled cast iron (ICCI) which is called as "Ni-hard". The Ni-hard cast iron contains $3-6\%$ Ni and $1.5-3\%$ Cr. Ni is a strong austenite stabilizer to restrain the pearlite transformation and promote the martensitic transformation of matrix in the as-cast state. In the Ni-hard cast iron, the wear resistance was improved because the hardness of eutectic M_3C carbide was

increased by alloying with Cr to form $(FeCr)_3C$ or M_3C carbide, as well as the hardness of matrix, was increased by adding a large amount of Ni for martensite transformation in the as-cast matrix. However, a considerable amount of austenite is remained in the as-cast structure due to the Ms temperature lowered by Ni. It was noted that an excess of retained austenite (γ_R) was injurious because it promoted spalling wear. In the case of a roll, therefore, the research and development of the other type of material were demanded.

High Cr cast iron was developed in 1970's. In high Cr cast iron, toughness was improved more and hardness was also increased much more than both of Ni-hard cast iron. The addition of Cr ranging 12-30% formed the $(CrFe)_7C_3$ or M_7C_3 carbides as a eutectic. The M_7C_3 carbide is much higher in hardness than M_3C carbide. The morphology of eutectic M7C3 carbide is not ledeburitic but the rod-like shape and in addition, the eutectic carbides were interconnected. This morphology gives more toughness than that of ledeburite in Ni-hard cast iron. Moreover, the matrix of high Cr cast iron could be improved widely by the heat treatment. From this reason, the high Cr cast iron has been used for a long time as materials for rolling mill rolls and those for pulverizing mill rolls in mining, cement, and steel making plants. However, the development of roll materials with higher performance than the high Cr cast iron was demanded in Japanese steel makers. On the 1990's, the multi-alloyed or multi-component white cast iron was invented by Matsubara research group collaborating with Nippon steel corp.[1].
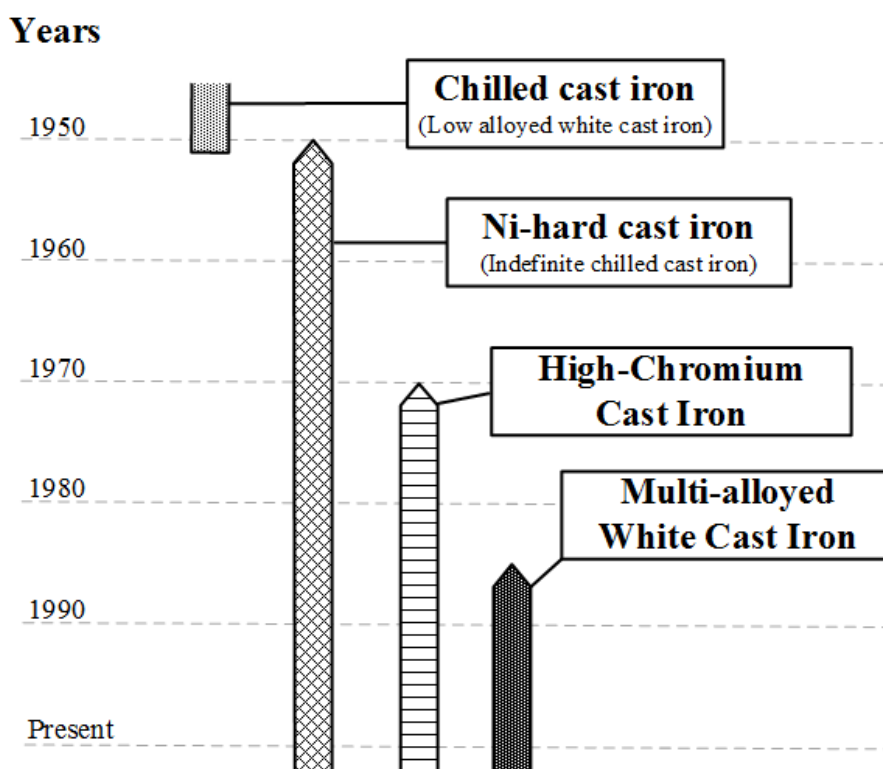
Fig. 1-1 Development and transition of cast iron materials for rolls [1].

Multi-alloyed white cast iron is a new type of alloyed white cast iron containing several kinds of strong carbide forming elements namely chromium (Cr), molybdenum (Mo), vanadium (V) and tungsten (W). This white cast iron has been widely applied to materials of work rolls of hot strip mills in steel making industry and some parts and components of pulverizing mills in cement industry. In typical microstructure of the multi-alloyed white cast iron, plural kinds of complex carbides such as MC, M_2C, M_6C and M_7C_3 precipitate as eutectic together with the matrices consisting of austenite, bainite, and/or martensite included secondary carbides. It is known that the type and amount of carbides and the matrix structure are determined by the chemical composition of the cast iron and its heat treatment [1-3]. Compared with conventional roll materials such as Ni-hard cast iron and high Cr cast iron, the multi-alloyed white cast iron shows superior abrasive wear resistance, high quality, and long service life in spite of less volume fraction of eutectic carbides [1, 4]. In the steel making industries, most of the hot strip mill rolls made of high Cr cast iron were replaced with rolls made of multi-alloyed white cast irons [1, 2, 5, 6].

The alloy composition of the multi-alloyed white cast iron was designed based on not only the type and morphology of eutectic carbide but also the phase transformation of the matrix. The basic alloy composition is 5 wt% (as shown by %) of each carbide forming elements, Cr, Mo, W, V and with 2%C [5, 7, 8]. Cobalt (Co) is not a carbide former but added to improve corrosion resistance, high-temperature strength, and thermal stability [5, 9]. The solidification sequence of the cast iron with basic alloy composition begins with crystallization of primary austenite (γ_p), followed by eutectic reaction of austenite and carbide [7, 8, 10]. The carbide forming elements also dissolve into matrix and effect on the phase transformation. In the heat treatment,

high temperature austenite transforms to bainite and/ or martensite depending on the kind and amount of alloying element and cooling rate [2, 5, 11]. The mechanical and wear properties of multi-alloyed white cast irons depend also on kind, amount of carbides and the matrix structure which differs from the heat treatment. In order to obtain desired properties, therefore, this cast iron must be heat-treated.

Generally, the hardening and tempering are given to the multi-alloyed white cast iron in the same way as steels and general cast irons [12]. While the alloyed cast iron is held at high temperature, retained austenite (γ_R) is destabilized by the precipitation of secondary carbides. Subsequently, the austenite transforms to bainite and/ or martensite during hardening. During tempering, not only the precipitation of special carbides occurs by the carbide reaction from martensite but also the retained austenite (γ_R) in the as-hardened state is decomposed to precipitate carbides and the rest of austenite transform into martensite during post cooling.

Molybdenum (Mo) is one of strong carbide formers and forms M_2C eutectic carbide with higher hardness than chromium carbide like M_7C_3 type. Besides, a certain amount of Mo is distributed into austenite and improves hardenability of the cast iron. It is well known that Mo promotes the precipitation of secondary carbides during heat treatment. Therefore, an addition of Mo is very useful for multi-alloyed white cast iron.

Nowadays, multi-alloyed white cast irons have been widely applied to the rolling mill rolls and began to employ the parts of machines in the cement and mining industries [1]. It was reported that the rolling mill rolls made of multi-alloyed white cast iron showed higher quality and performance and they increased the service life 3-5 times as long as the conventional rolls made of Ni-hard and high Cr cast irons

[1, 2, 5]. Unquestionably, the application of this kind of cast iron will be expanded increasingly to many industrial fields in near future. From these viewpoints, the research on heat treatment behavior of multi-alloyed white cast iron is very significant and helpful for more practical applications.

Looking back the last 30 years, the research and development on the multi-alloyed white cast irons have been carried out systematically on solidification sequence and phase transformation using the basic alloy composition [8, 11]. However, the systematic research on the behavior of heat treatment, i.e., a variation of hardness and retained austenite (γ_R) of the cast iron varying the alloy content was a quite few. From these viewpoints mentioned in Introduction, the following research was performed systematically.

1.2 Objective of Research

The objective of this research is to clarify the effect of Mo content on heat treatment behavior of multi-alloyed white cast irons having basic alloy composition (2%C-5%Cr-5%W-5%V-2%Co). The Mo content of the specimen are varied from nil to 7.7% and the investigation focuses on the variation of hardness, the volume fraction of retained austenite (Vγ) and their correlations associated with Mo content and heat treatment conditions.

1.3 Scopes of research

The experiments will be carried out as follows;

1. Heat treatment of annealing at 1,223 K (950 °C), austenitizing at 1,373K (1,100 °C) and tempering at 673-873 K (400-600 °C) by 50 K (50 °C) intervals.

2. Measurement of macro- and micro- hardness in the as- cast and the heat-treated states.

3. Measurement of volume fraction of retained austenite (Vγ) in the as-cast and the heat-treated states.

4. Investigate of microstructures by Optical Microscope (OM) and Scanning Electron Microscope (SEM).

5. To clarify the effect of Mo content on behaviors of hardness and Vγ during heat treatment.

1.4 Advantage of research

1. This research clarifies the effect of Mo content on heat treatment behavior in relation to hardness, the volume fraction of retained austenite (Vγ) and microstructures.

2. This research can provide important data for the practical heat treatment to improve the mechanical properties and abrasive wear resistance.

3. This research can contribute to expanding the further practical applications of multi-alloyed white cast iron in the other fields of industries in near future.

Chapter II

Literature Reviews

It is known that high Cr cast iron has been used as not only rolling mill roll materials but also materials for parts or components of many kinds of machine for a long time because of its high abrasion wear resistance [1, 5]. In order to upgrade the productivity, a new type of alloyed cast iron with higher wear resistance and performance was developed. In the improvement of high Cr cast iron, small amount of strong carbide formers such as Ti, Nb, V and Mo which form secondary carbides with high hardness in the matrix, were tried to add in the cast iron. The types and the hardness of carbides and matrix are shown in Table 2-1 [13]. However, it was aimed to improve the heat treatment behavior of matrix. Later, relatively large amount of such alloying elements were added to crystallize their own eutectic carbides during solidification.

Multi-alloyed white cast iron was developed in Japan about 30 years ago by Y. Matsubara and his colleagues collaborating with the roll group of Nippon Steel Corporation [5]. This cast iron has plural and different eutectics in the microstructure and has been being of widely applied to work roll materials and parts of machines because of excellent abrasive wear resistance and high strength at elevated temperature [2, 4, 14, 15]. The multi-alloyed white cast iron has been designed in complex alloy system of Fe-X-C where X means plural strong carbide forming elements such as V, Cr, W, and Mo. These elements form special types of carbides such as MC, M_2C, M_6C and M_7C_3 with extremely high hardness [2, 3]. Such carbide forming elements also

dissolve into matrix and affect to the phase transformation of the matrix, especially heat treatment behavior.

The scheme in the research and development of multi-alloyed white cast iron began to alloy design and developed to solidification, phase transformation, heat treatment and abrasive wear behaviors.

Table 2-1 Hardness of carbides and matrix phases [10, 13, 16].

Carbide or matrix	Hardness (HV)
Fe_3C	800-1,100
$M(FeCr)_7C_3$	1,200-1,800
$M(CrFe)_{23}C_6$	850-1100
Mo_2C	1,500
$M(MoFe)_6C$	1,800-2,200
WC	2,400
W_2C	3,000
$M(FeW)_6C$	1,900-2,100
VC	2,600-2,850
TiC	3,200
NbC	2,400
Ferrite	70-200
Pearlite	250-320
Pearlite (alloyed)	300-460
Austenite (low alloy)	300-600
Martensite	500-1,000

2.1 Alloy design

The chemical composition of the multi- alloyed white cast iron has been designed by consideration of not only the type and morphology of carbide crystallized from the liquid but also the transformation behavior of matrix by heat treatment. The main purpose is to improve the abrasion wear resistance by introducing hard special eutectic carbides and matrix strengthened with secondary precipitation of hard carbides.

V is strongest carbide former in the list of candidate elements. It combines with C to form (V, Fe)C or MC carbide during solidification. The MC carbide has high hardness than chromium carbide $(Cr, Fe)_7C_3$ or M_7C_3 and this leads to improve hardness and wear resistance [1, 5]. In addition, V decreases size of eutectic carbide which could be expected to improve the toughness of cast iron. However, V decreases hardenability during heat treatment by promoting pearlite transformation [17, 18]. It was reported that V promoted the precipitation hardening during tempering due to the carbide reaction. Therefore, it can be said that V is the most favorable alloying element added in multi-alloyed white cast iron.

Mo and W are also strong carbide forming elements and form M_2C or M_6C carbide. It was reported that Mo tends to stabilize the M_2C carbide while W tends to form M_6C carbide [16]. These carbides have higher hardness than chromium carbides of M_7C_3 and $M_{23}C_6$. Besides, Mo increases strength and improves the hardenability of the cast iron [1, 4, 5]. Mo increases the amount of retained austenite because it lowers the Ms temperature [19, 20]. Both of Mo and W promote the secondary precipitation hardening of matrix by tempering [1, 4, 5]. Since Mo and W have similar lattice parameter and used to form the similar type of carbide, they show similar action in the cast iron. As the atomic weight of Mo is about a half of W, a parameter of tungsten

equivalent (W_{eq}) can be introduced to evaluate the total effect of Mo and W. The W_{eq} is expressed by the following equation.

$$W_{eq} = 2\%Mo + \%W \tag{2.1}$$

There is a report that the fracture toughness of the cast iron was reduced when W_{eq} was about 10-11% [4].

Cr is a carbide forming element and forms M_7C_3 and $M_{23}C_6$ types. These carbides show good abrasion wear resistance. Cr increases the hardenability of the cast iron because Cr shifts pearlite transformation to the long time side [12]. It was reported that an increase in Cr content refines the eutectic structure by reducing the eutectic freezing range [12, 15]. The M_2C carbides could precipitate when the Cr/C value about 5. By contrast, the precipitation of M_6C carbides took place when Cr/C value was about 10 [19].

C is the main element in the cast iron that influences on the formation and amount of carbide and matrix structure. The role of C is divided to two, formation of eutectic carbides during solidification and dissolution of the remainder into matrix. In the multi-alloyed white cast iron, there are plural types of carbides crystallized as eutectics. Here, the carbon balance (C_{bal}), which is defined as a parameter to express the behavior of C dissolving in the matrix, is introduced and it is shown by the next equation [5, 14].

$$C_{bal} = \%C - C_{stoich} \tag{2.2}$$

where %C is the C content of the cast iron and the C_{stoich} is the amount of C which combines all with carbide forming elements to form their own carbide. The C_{stoich} value can be theoretically calculated using the following equation [5, 14].

$$C_{stoich} = 0.060\%Cr + 0.033\%W + 0.063\%Mo + 0.235\%V \tag{2.3}$$

This equation is valid when M_7C_3 eutectic carbide does not precipitate in the cast iron [5]. In the case that M_7C_3 eutectic exist in the structure, on the other side, the C_{stoich} must be calculated by the next equation.

$$C_{stoich} = 0.099\%Cr + 0.033\%W + 0.063\%Mo + 0.235\%V \qquad (2.4)$$

In the view point of heat treatment, the C_{bal} is a very important factor. The C_{bal} determines the amount of C dissolved in the matrix more or less than equilibrium state. A positive C_{bal} value means that an excess of C remains in the matrix. By contrast, a negative C_{bal} value means that very little C is left in the matrix. As for the hot work roll, the MC and M_2C carbides are preferred. The C_{bal} from equation 2.3 should be kept near 0% [5].

Cobalt (Co) is not a carbide forming element but most of Co distributes to matrix and then, it affects the phase transformation of matrix, say a decrease in hardenability. Even that, the Co is added to multi-alloyed white cast iron for improvement of the strength at high temperature and that of the resistance to softening due to tempering and the coarsening of grains [5, 6].

2.2 Carbides in multi-alloyed white cast iron

The several types of carbides exist in multi-alloyed white cast iron. They show a diversity of morphology depending on the chemical composition. The type and morphology of carbide in multi-alloyed white cast iron was already studied and the following results were clarified.

MC carbide contains more than 50%V and it precipitates as eutectic carbides during solidification. The MC carbide is classified into petal-like, nodular and coral-like morphologies as shown in Fig. 2-1. The change in morphology of MC carbide

according to the V and C contents in multi-component white cast iron was reported using the alloy of Fe-5%Cr-2%Mo-2%W-5%Co by Wu et.al [21] and they are shown in Fig 2-2. The eutectic MC carbide in petal-like morphology precipitates in a low C cast iron. By contrast, eutectic MC carbide in nodular shape precipitates in the cast iron with high C content. The structure of MC carbides shown in Fig. 2-1 (c) consists of primary large MC crystals and eutectic MC carbide in granular shape. The three-dimensional morphology of this eutectic shows in a coral-like morphology and they precipitated in the cast iron with high V content. The hardness of MC carbide is about 2,600-2,850 HV [10, 16]. It was reported that the MC carbide is very effective to the abrasive wear resistance of the cast iron [5]. MC carbide with nodular morphology will improve the toughness because of less notch effect [5, 22].

(a) Petal-like

(b) Nodular

(c) Coral-like
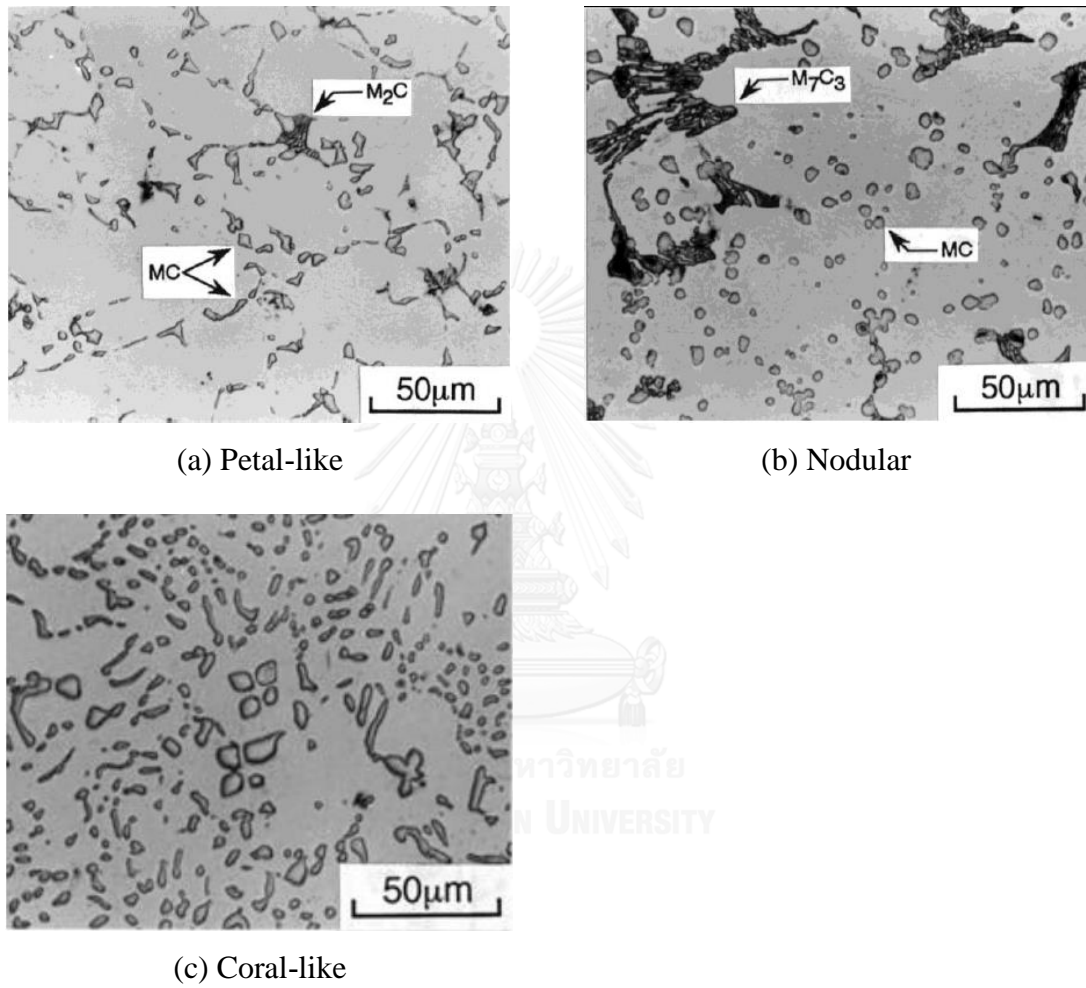
Fig. 2-1 Two-dimensional microstructures of MC carbide [5].
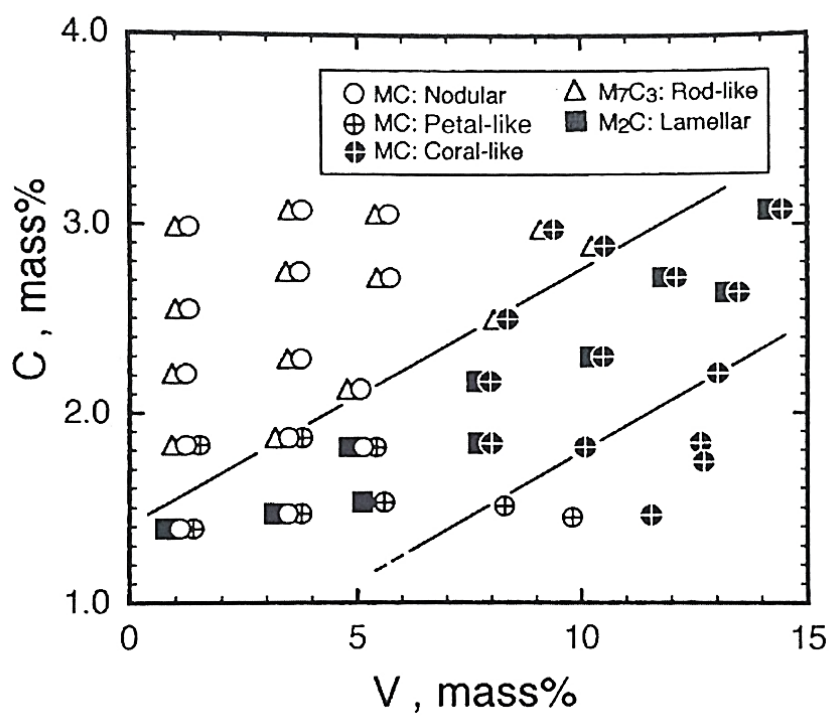
Fig. 2- 2 Influence of V and C content on the type and morphology of carbide crystallized from the liquid during solidification of multi- component white cast iron. (Base alloy: Fe-5%Cr-2%Mo-2%W-5%Co) [21].

M$_2$C eutectic solidifies finally in the liquid enriched with Mo and W [2, 5, 7]. This carbide can be classified into two types, fine lamellar and coarse plate- like morphologies, as shown in Fig. 2-3. The M$_2$C carbide could transform into M$_6$C carbide during heat treatment [23]. The effect of W$_{eq}$ value and C content on morphology of M$_2$C carbide in multi-component white cast iron with 5% each of Cr, V and Co is shown in Fig. 2-4. The plate-like M$_2$C carbide is observed in the cast iron with more than 15% of W$_{eq}$. The plate- like M$_2$C carbide usually precipitate together with M$_7$C$_3$ carbide in the cast iron with high C content. The fine lamellar M$_2$C carbide is found to precipitate in the cast iron with low W$_{eq}$ and low C content. The hardness of M$_2$C carbide is 1,800-2,200 HV [6, 10, 16, 24].
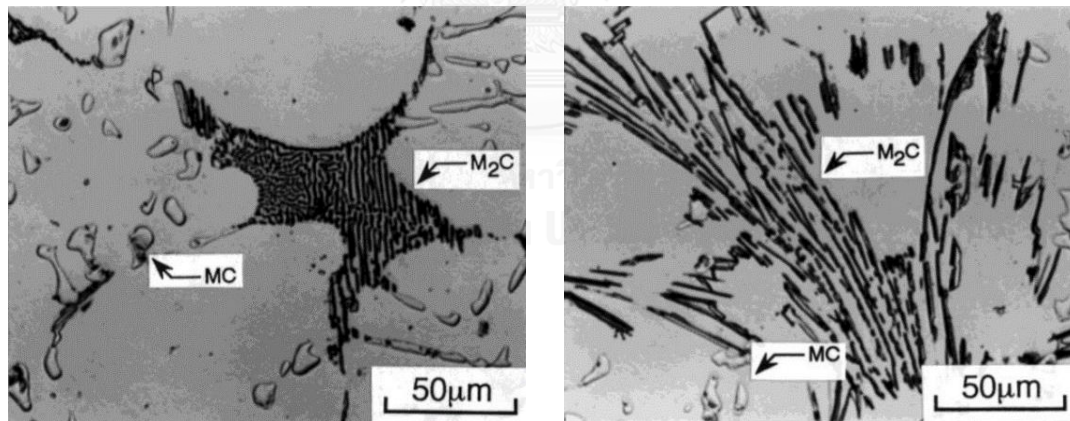
(a) lamellar   (b) Plate-like

Fig. 2-3 Two-dimensional microstructures of M$_2$C carbide [5].
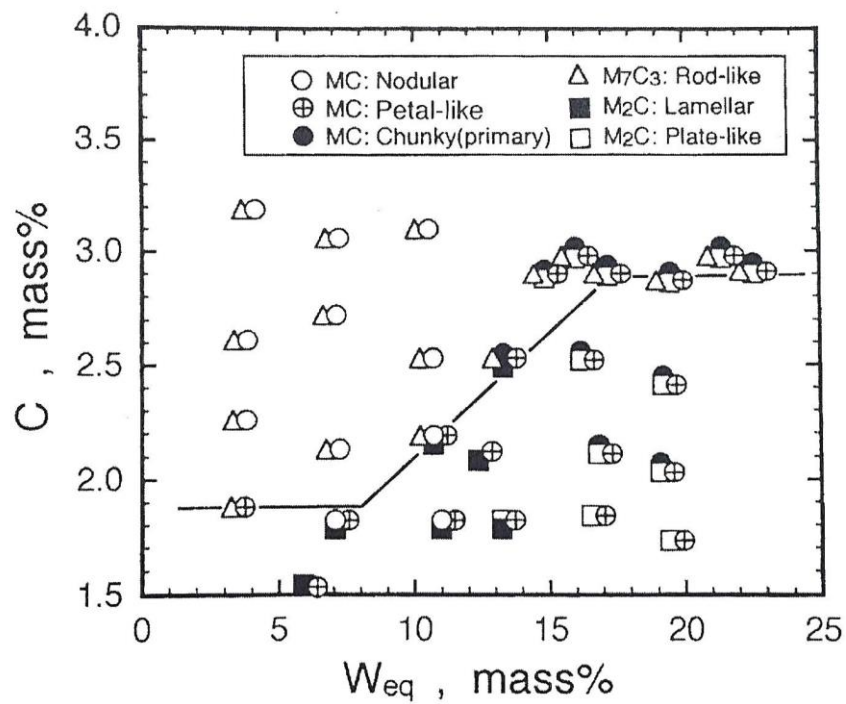
Fig. 2-4 Influence of W_{eq} value and C content on type and morphology of carbide crystallized from the liquid during solidification of multi- component white cast iron. (Base alloy: Fe-5%Cr-5%V-5%Co) [21].

M$_6$C carbide has a different crystal structure and alloy concentration from M$_2$C carbide. The M$_6$C carbides with a face-centered cubic lattice precipitate as eutectic in a fish-bone morphology along the grain boundary. It is composed of Mo, W, Cr and Fe [4, 7, 25]. Mostly, M$_6$C carbide precipitates as spheroid in the matrix after heat treatment and this may lead to improving the toughness and wear resistance. Fig. 2-5 shows schematic explanation for the decomposition processes of M$_2$C eutectic carbide to M$_6$C carbide. The reactions can be displayed by the following equations [23].

$$M_2C + \gamma\text{-iron} \rightarrow M_6C \qquad\qquad (2.5)$$

$$M_6C + \gamma \rightarrow M_6C + MC \qquad\qquad (2.6)$$

$$M_2C + \gamma \rightarrow M_6C + MC + M_7C_3 \qquad\qquad (2.7)$$
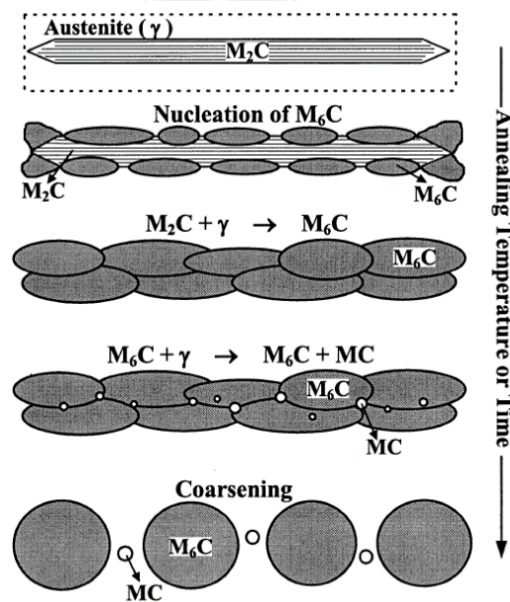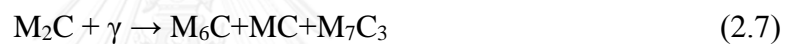
Fig. 2-5 Schematic explanation for decomposition processes of M$_2$C carbide to M$_6$C carbide [23].

The M_7C_3 carbide shows rod-like structure that is similar to high Cr cast iron as shown in Fig. 2-6. Sometimes, it co-exists with MC and M_2C carbides in the cast iron with high W_{eq} and high C contents [5]. The hardness of M_7C_3 carbide is 1,200-1,800 HV [4, 16, 24].
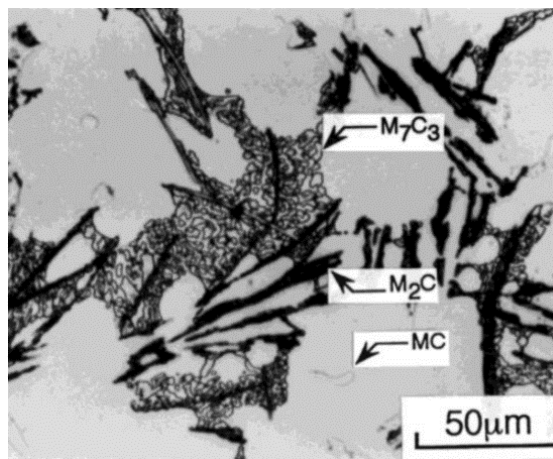
Fig. 2-6 Two-dimensional microstructure of M_7C_3 eutectic carbide [5].

The effect of solidification rate (R_E) and C content on the type of eutectic carbide in the multi-component white cast iron with basic alloy of 5%Cr-5%Mo-5%W-5%V-5%Co is shown in Fig. 2-7. It is found that the MC and M_2C carbides precipitate at all the range of C content and the rate of eutectic growth. However, M_7C_3 carbide precipitates only in the specimens with C content higher than 2.5%, while the M_3C could precipitate in the specimens with more than 3%C and low eutectic growth rate.
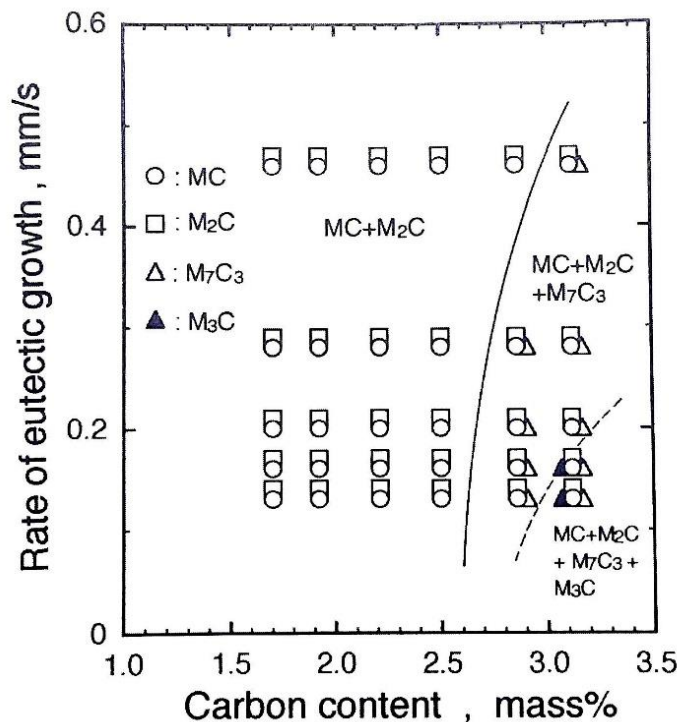
Fig. 2-7 Types of carbides in as-cast microstructure corresponding to carbon content and eutectic growth rate of multi-alloyed white cast irons [5].

2.3 Solidification sequence

Solidification sequence of multi- alloyed cast iron with basic chemical composition (Fe- 5%Cr- 5%Mo- 5%W- 5%V- 5%Co- 2. 0%C alloy) was studied by Matsubara et. al using quench tests during thermal analysis. Fig 2- 8 (a) shows a thermal analysis curve and Fig 2-8 (b) shows the transition of microstructure when the melt was quenched into the water from given temperatures [5]. The solidification sequence can be explained as follows.

First of all, the primary austenite dendrite crystallizes in the liquid, followed by the precipitation of (γ + MC) eutectic and finally, the (γ + M_2C) eutectic solidifies. The solidification sequence of this alloy is expressed by the next equations,

$$L_0 \rightarrow \gamma_p + L_1 \qquad\qquad \text{at 1590 K}$$

$$L_1 \rightarrow (\gamma + MC)_E + L_2 \qquad\qquad \text{at 1558 K}$$

$$L_2 \rightarrow (\gamma + M_2C)_E \qquad\qquad \text{at 1422 K}$$

(a) Thermal analysis curve   (b) Quenched microstructure
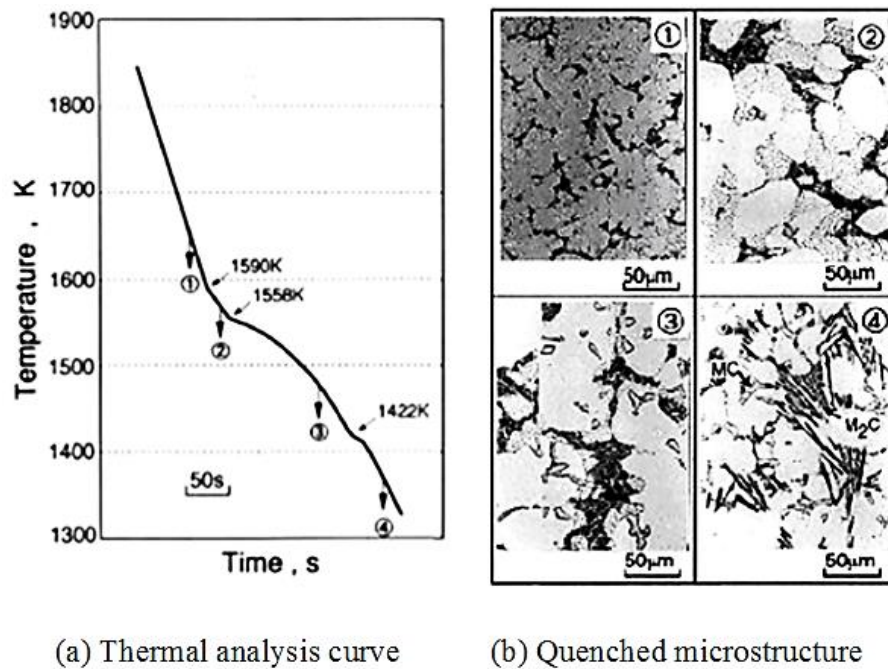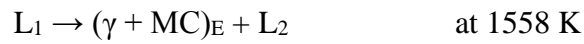
Fig. 2-8 Thermal analysis curve showing quenching positions or temperatures (a), and transition of microstructures corresponding to quenched positions (b). (Fe-5%Cr-5%Mo-5%W-5%V-5%Co-2%Co alloy) [21]

There is a research reported on the solidification sequence for multi-alloyed white cast irons with different combination of alloy contents. Their solidification sequences are summarized in Table 2-2.

The types of eutectic carbides precipitated in each multi-component white cast iron are also shown in the table. From lots of quench tests, Wu et. al proposed a quasi-binary phase diagram at high temperature area of multi-alloyed white cast iron

with basic alloyed composition, and it is shown in Fig. 2-9. This diagram has a eutectic reaction of $(\gamma+MC)$ at about $2.8\%C$. However, two other eutectic reactions lie in lower temperature region than the $(\gamma+MC)$ eutectic, $L \rightarrow \gamma+M_2C$ and $L \rightarrow \gamma+M_7C_3$ of which reactions occur depending on the C content [2, 5, 7]. It is found that this phase diagram is very useful to predict the solidification sequences of multi-alloyed white cast iron.

Table 2-2 Solidification sequences of multi-alloyed white cast irons with different chemical compositions [5].

Number	Chemical composition	Combination of carbide	Solidification Sequence	
1	2%C-5%Cr -2%Mo-2%W -9%V-5%Co	Coral-like MC- Lamellar M_2C	$L_0 \rightarrow \gamma_p+L_1$ $L_1 \rightarrow (\gamma+MC)_E+L$ $L_1 \rightarrow (\gamma+MC)_E+L_2$	at 1651 K at 1631 K at 1498 K
2	3%C-5%Cr -2%Mo-2%W -5%V-5%Co	Nodular MC- Rod-like M_7C_3	$L_0 \rightarrow \gamma_p+L_1$ $L_1 \rightarrow (\gamma+MC)_E+L_2$ $L_1 \rightarrow (\gamma+M_7C_3)_E+L_2$	at 1556 K at 1515 K at 1452 K
3	3%C-5%Cr -2%Mo-2%W -9%V-5%Co	Chunky and coral-like MC Rod-like M_7C_3	$L_0 \rightarrow \gamma_p +L_1$ $L_1 \rightarrow (\gamma+MC)_E+L_2$ $L_1 \rightarrow (\gamma+M_7C_3)_E+L_2$	at 1732 K at 1550 K at 1453 K
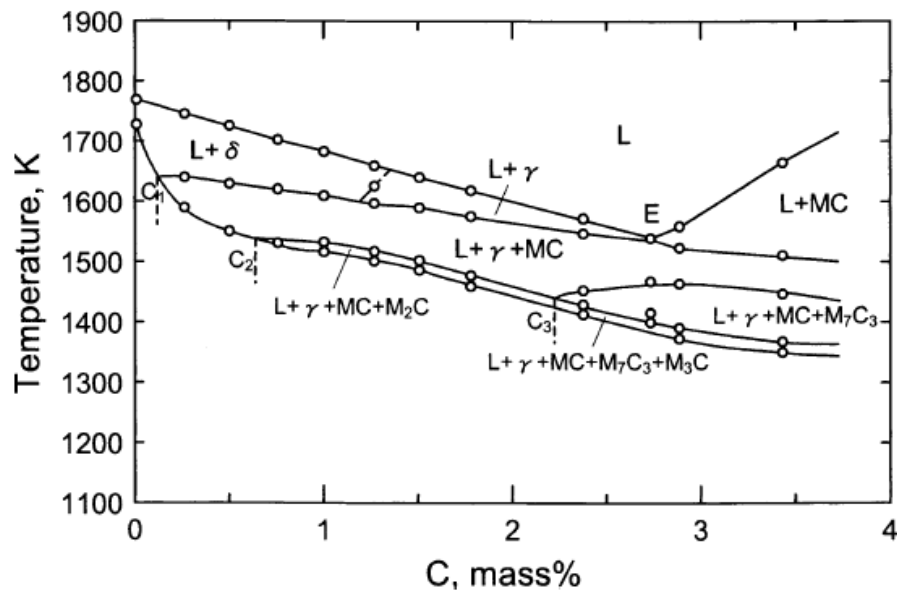
Fig. 2-9 Quasi-binary phase diagram for M (Fe-5%Cr-5%V-5%Mo-5%W-5%Co)-C

system [5].

2.4 Heat treatment behavior

There are many papers concerning the heat treatment of high Cr cast irons. As- cast microstructure of alloyed white cast iron varies depending on chemical composition and cooling rate. There exist martensite, bainite or pearlite and austenite in the as-cast matrix [14, 19, 26]. It is considered that pearlitic matrix provides naturally poor abrasive wear resistance [14]. In high Cr cast iron, an excess of retained austenite (γ_R) makes the hardness low and leads to reduce the abrasive wear resistance [12, 26]. The highest abrasive wear resistance in the high Cr cast iron was obtained when the matrix was martensite [26]. In the case that multi- alloyed white cast iron is practically applied to hot rolling mill rolls, the retained austenite (γ_R) is undesirable because it may transform into martensite during operation and consequently, it leads failure of roll, say cracking and/or destruction. In order to get the high wear resistance

by using the multi-alloyed white cast iron, however, the cast iron must be heat-treated to obtain the optimum combination of hardness and retained austenite (γ_R).

The behavior of phase transformation during continuous cooling from high temperature austenite was investigated using a computer controlled dilatometer and then, many kinds of continuous cooling transformation (CCT) curves have been made by Yokomiso et.al. [5]. The CCT diagrams of low and high C multi-alloyed white cast irons cooled from austenitizing temperatures of 1,273K and 1,373K were reported and they are shown in Fig. 2-10 (a) and (b), respectively. In spite of the difference in C content, pearlite and bainite transformations branched away to the top and the bottom independently. The noses of pearlite and bainite range from 900-980 K and 570 to 640K, respectively. When the austenitizing temperature is elevated to 1373K, both of the transformations are delayed approximately twice. The temperature to start the martensite transformation (Ms) appears at 400-500 K in low C cast iron while, in high C cast iron, it lowers than 400K. This reason is explained that an enrichment of C in austenite caused by elevating the austenitizing temperature and decreased the Ms temperature.

(a) 1.95 %C   (b) 2.81 %C
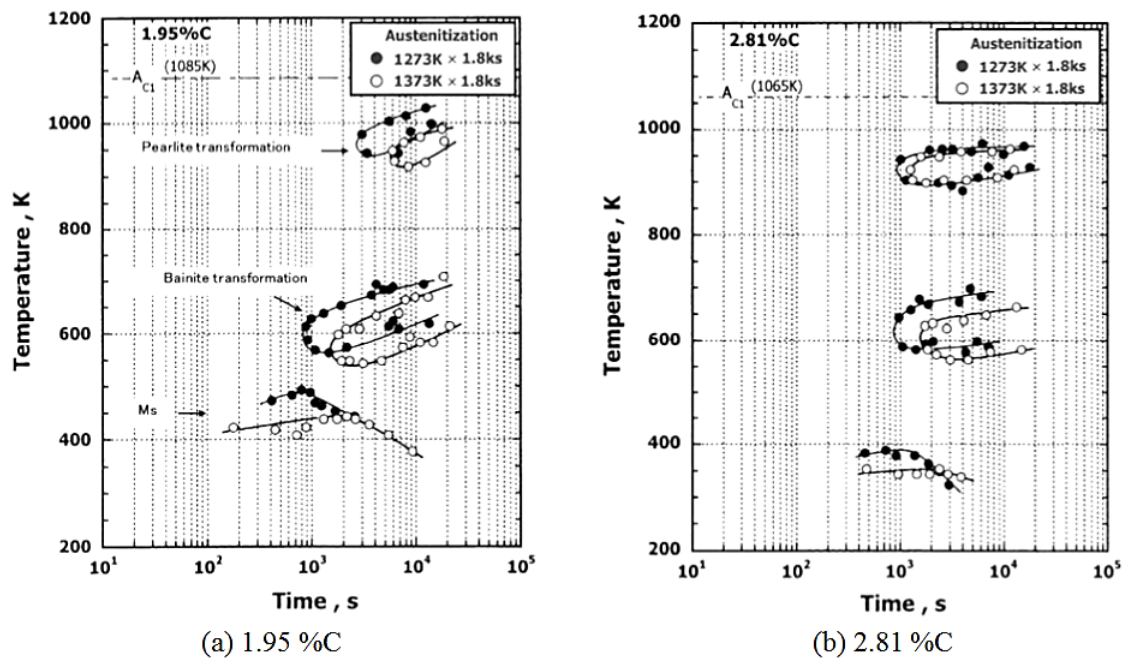
Fig. 2- 10 Continuous cooling transformation (CCT) curves of multi- alloyed white cast irons with different C content in basic alloy composition [2, 5].

As for the research on heat treatment of high Cr cast iron, "Effect of alloying elements on heat treatment behavior of hypo eutectic high Cr cast iron" was published by Sudsakorn et. al. In the paper, it was described that the tempered hardness rose as Mo content increased while other elements showed negative effect [12].

Presently, the published paper which in researched systematically on the heat treatment of multi-alloyed white cast iron is only on effect of C content by Wannaporn et. al [27] and Co content by Sasaguri et al [9]. As shown in Fig. 2-11 (a), the hardness decreases with increasing of Co content in the as-cast and annealed states but changed little in as-hardened state. In the tempered state shown in Fig. 2-11 (b), however, the maximum hardness (H_{Tmax}) was obtained at a certain temperature and H_{Tmax} increased markedly with an increase in Co content. These results suggest that Co promotes the secondary hardening due to the precipitation of special carbides and then, increases the matrix hardness.

(a) As-cast, as-annealed and as-hardened states
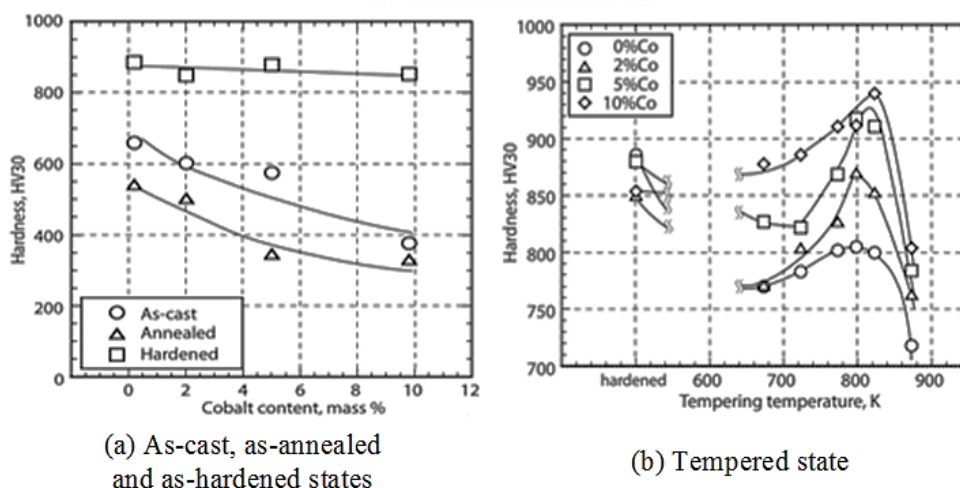
(b) Tempered state

Fig. 2-11 Effect of Co content on the hardness in as-cast, annealed, as-hardened states (a) and tempering hardness curves (b) of multi-alloyed white cast iron with basic alloy composition [9].

And " Effect of C content on heat treatment behavior of multi- alloyed white cast iron for abrasive wear resistance" was published by Jatupon et. al [28]. In the results of his studies shown in Fig. 2-12 (a) and (b), the tempered hardness curves show an evident secondary hardening. In the same way, the Vγ is increased as the C content increases. On the other hand, the Vγ in each cast iron was decreased as the tempering temperature increases. In the specimens with 2.00%C and 2.34%C, the Vγ decreases greatly when the tempering temperature gets over 723K.

(a) 2.00%C   (b) 2.34%C
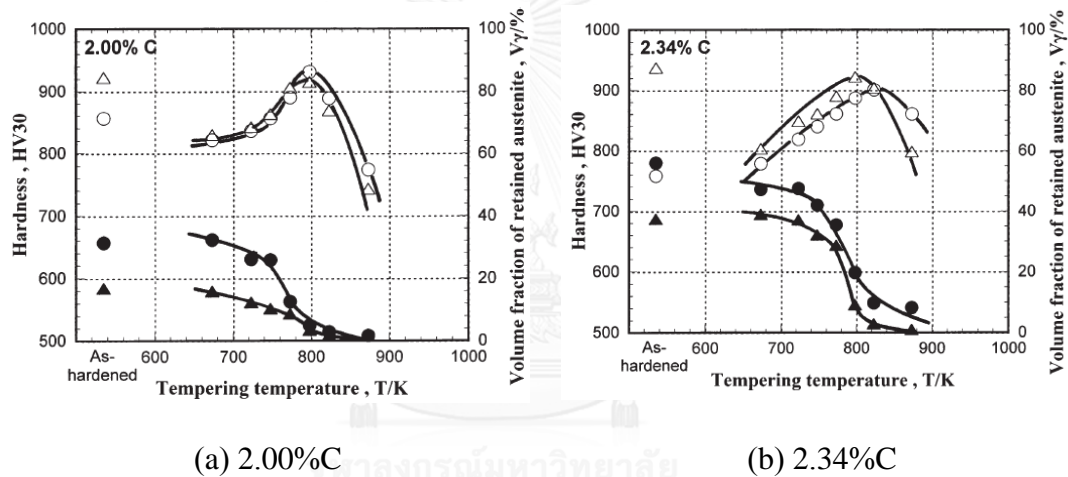
Fig. 2-12 Effect of C content and tempering temperature on the heat treatment behavior

of multi-alloyed white cast iron with (a) 2.00%C and (b) 2.34%C [28].

Chapter III

Experimental procedures

3.1 Preparation of test specimens

The charge calculations were carried out to obtain the target chemical compositions of test specimens using raw materials such as steel scrap, pig iron, ferro-alloys and pure metals. The charge materials were melted in a high-frequency induction furnace with 30 kg capacity. The melt was superheated to 1,853 K (1,580 °C). After being held for 10 to 15 min., the melt was poured at 1,773-1,793 K (1,500-1,520 °C) into preheated CO_2 bonded sand molds in a round bar shape with cavity size of 25 mm in diameter and 65 mm in length. The schematic drawing of the mold is shown in Fig. 3-1. Instantaneously, the melt in the riser is covered by dry exothermic powder to prevent the melt from fast cooling. The chemical compositions of specimens are summarized in Table 3-1. The round bar specimens were cut out by a wire-cutting machine to obtain the test piece in disk shape with 7 mm in thickness.
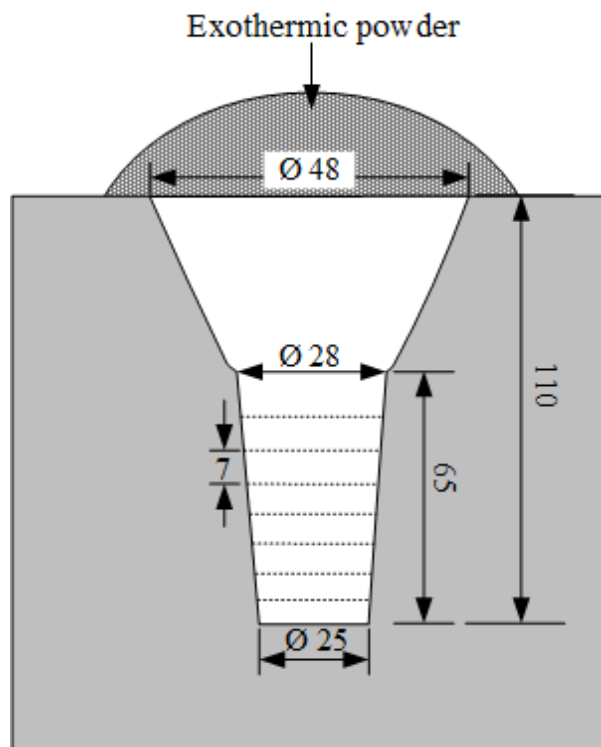
Fig. **3-1** Schematic drawing of CO_2 bonded sand mold for making round bar specimen.

Table 3-1 Chemical compositions of test specimens.

Specimen No.	Element (wt%)								W_{eq}	C_{bal}
	C	Si	Mn	Cr	Mo	W	V	Co		
No.1	2.05	0.51	0.48	5.13	0.12	4.95	5.09	1.99	5.00	0.38
No.2	2.08	0.47	0.48	5.09	1.17	4.92	5.03	2.01	7.00	0.36
No.3	2.09	0.52	0.50	5.11	3.02	5.06	5.10	2.01	11.00	0.24
No.4	2.00	0.53	0.49	4.96	4.98	4.98	5.01	2.03	15.00	0.07
No.5	2.06	0.50	0.47	5.00	7.66	4.98	5.01	1.98	20.00	-0.04

Note : $W_{eq} = 2\%Mo + \%W$

$C_{bal} = \%C - (0.06\%Cr + 0.033\%W + 0.063\%Mo + 0.235\%V)$

3.2 Heat treatment

The conditions of heat treatment process are shown in Table 3-2. The test pieces coated with an anti-oxidation solution to prevent oxidation and decarburization were supplied to annealing. In annealing process, the specimens were heated to 1,223 K (950 °C) in an electric furnace and held there for 18 ks and then, cooled in the furnace to room temperature. For hardening, the annealed specimens were austenitized at 1,373 K (1,100 °C) for 3.6 ks in a vacuum furnace. The pressure in the furnace was controlled at about 0.05-0.07 Pa. While the specimens were held at austenitizing temperature, however, the pressure was preserved at about 250 Pa. After austenitizing, the test pieces were quenched by a cooled gas nitrogen using Cold Evaporator (CE), which can store up the liquid nitrogen at extremely low temperature. The evaporated nitrogen gas was jet-sprayed to the test pieces under the pressure of 400 kPa. The hardened test pieces were tempered at 673-873 K (400 - 600 °C) at 50 K intervals for 12 ks in an electric furnace and cooled to room temperature in still air.

Table 3-2 Heat treatment processes and conditions.

Heat treatment	Temperature (K/°C)	Holding Time (ks)	Cooling Condition
Annealing	1223/950	18	Furnace Cooling (FC)
Austenitizing	1373/1100	3.6	N_2 Quench (N_2Q)
Tempering	673/400 723/450 748/475 773/500 798/525 823/550 873/600	12	Air Cooling (AC)

3.3 Investigation of solidification microstructure

3.3.1 Thermal analysis

The equipment for thermal analysis is shown in Fig. 3-2. The 55 g of sample was re-melted in an alumina crucible using an electric furnace with SiC resistance under Ar gas atmosphere. The melt was heated up to 1,773 K (1,500 °C) and then, held for 15 minutes at the temperature. After holding, the melt was cool down to 1,223 K (950 °C) with approximate 0.3 K/s of cooling rate for thermal analysis. An R type thermocouples (②) were submerged into the melt to measure the cooling curve.

① Automatic Recorder
② R thermocouple
③ Argon gas inlet tube
④ Alumina tube
⑤ Alumina crucible
⑥ Graphite rod
⑦ Silicon carbide resistance furnace
⑧ Specimen
⑨ Slide plate for quenching
⑩ Cooling water
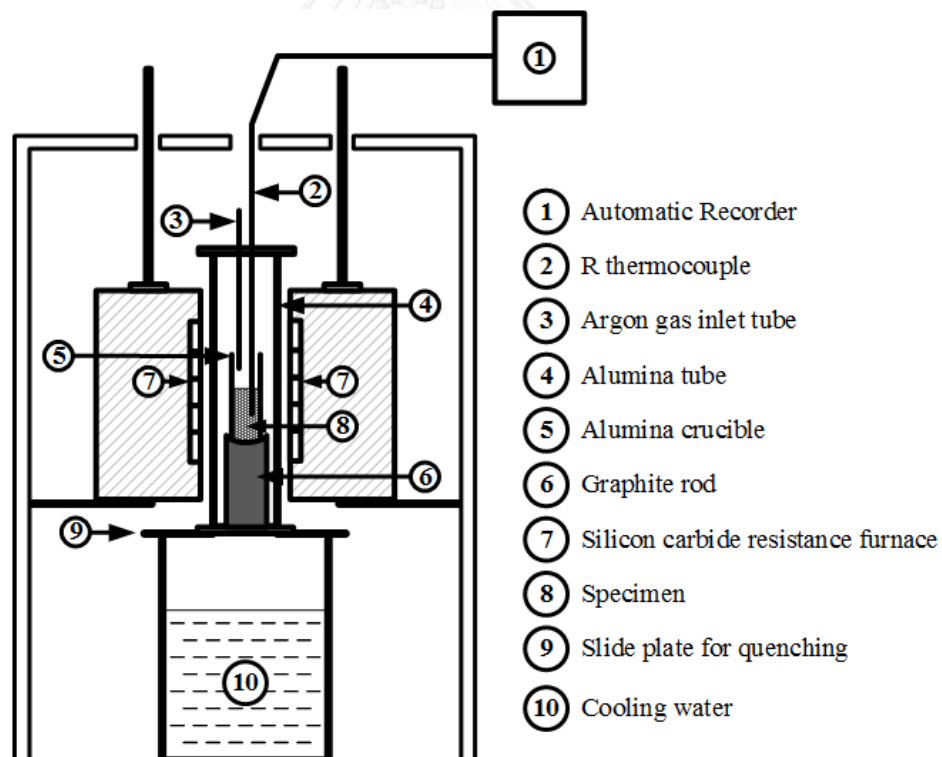
Fig. 3-2 Schematic drawing of equipment for thermal analysis.

3.3.2 Investigation of microstructure

3.3.2.1 Optical microscope (OM)

The microstructure of test piece was observed by an optical microscope (OM). The heat-treated test piece was polished using SiC emery papers in the order of 80, 120, 180, 320, 400, 600, 1,000 and 1,200 meshes and finally buffed with alumina powder of 0.3 micron in grain size. Etchants and etching method to reveal the microstructure are summarized in Table 3-3. The etchant type A (Murakami) was adopted to identify carbide type because carbides show different colors after etching. By contrast, the etchant type B (Villella) was generally used to reveal the matrix microstructure.

Table 3-3 Etchants and etching methods.

Type	Etchant	Etching method	Observation
A (Murakami)	KOH 10g K$_3$Fe(CN)$_6$ 10g Water 100 cc	Immersion at 60°C for 2 minute	Colored the carbide
B (Villella)	Picric acid 1 g HCl 5 cc Ethanol 95 cc	Immersion at room temperature	Microstructure

3.3.2.2 Scanning electron microscope (SEM)

Scanning electron microscope (SEM) was used to observe the detailed microstructure and morphology of carbide with high magnification. A polished test piece is etched by the etchant type B (Villella) to reveal the microstructure. The microphotographs of matrix were taken at magnification of 2,500 and 8,000, focusing on the matrix areas.

3.3.3 Measurement of volume fraction of retained austenite

The X-ray diffraction method was introduced to measure the volume fraction of retained austenite ($V\gamma$) quantitatively. A special goniometer with simultaneously automatic rotating and swinging sample stage was used to cancel the preferred orientation of austenite. The Mo-Kα characteristic line with the wave length of 0.007 nm (0.0711 A°) that was filtered by Zr foil was utilized as a source of the X-ray beam. The mirror polished specimen was attached to the sample stage and scanned the goniometer from 24 to 44 degree by 2θ. The four diffraction peaks on the chart, which were independent or not interfering from peaks of unnecessary phases, were selected for $V\gamma$ calculation. The diffraction peak-s adopted were (200) and (220) planes for ferrite (α) or martensite (M), and (220) and (311) planes of austenite (γ). The conditions of measurement are shown in Table 3-4. The $V\gamma$ was obtained by averaging the values calculated from the three combinations of peaks, α_{200} - γ_{311}, α_{200}–$\Sigma\gamma(220,311)$ and $\Sigma\alpha(200,220)$-γ_{311}.

Table 3- 4 Measurement conditions of volume fraction of retained austenite (V_γ) by X-ray diffraction method.

Target metal	Mo
Tube voltage – current	50 kV- 30 mA
Slits	Divergence slit: 1°, Receiving slit: 1.5 mm Scattering slit: 1°
Filter	Zr
Scanning range (2θ)	24-44 deg
Scanning speed	0.5 deg/min
Step/Sampling	0.01 deg

3.3.4 Analysis of alloying concentration by electron probe micro-analysis (EPMA)

In order to confirm the type of precipitated carbides in the matrix, the tempered test piece was etched by the etchant of type B Villella's reagent shown in Table 3-3. The alloy concentration of precipitated carbides in the matrix was analysed quantitatively using EPMA equipped with Energy Dispersive X-ray Spectroscopy (EDS).

3.4 Hardness measurement

Macro-hardness of the test piece was measured using Vickers hardness tester with a load of 294.2 N (30 kgf) and micro-hardness of matrix was performed using Micro-Vickers hardness tester with a load of 0.98 N (0.1 kgf). The measurement of hardness was carried out randomly at more than five points on a surface of test piece and the values were adopted.
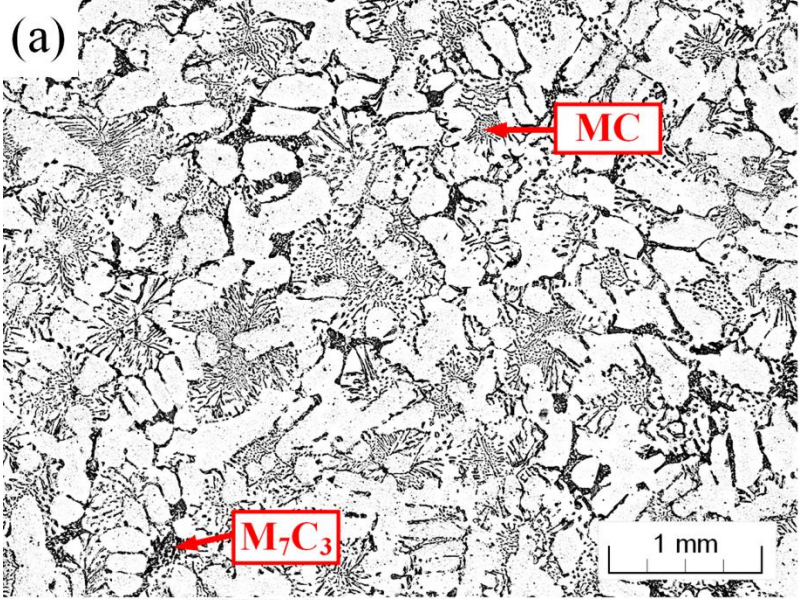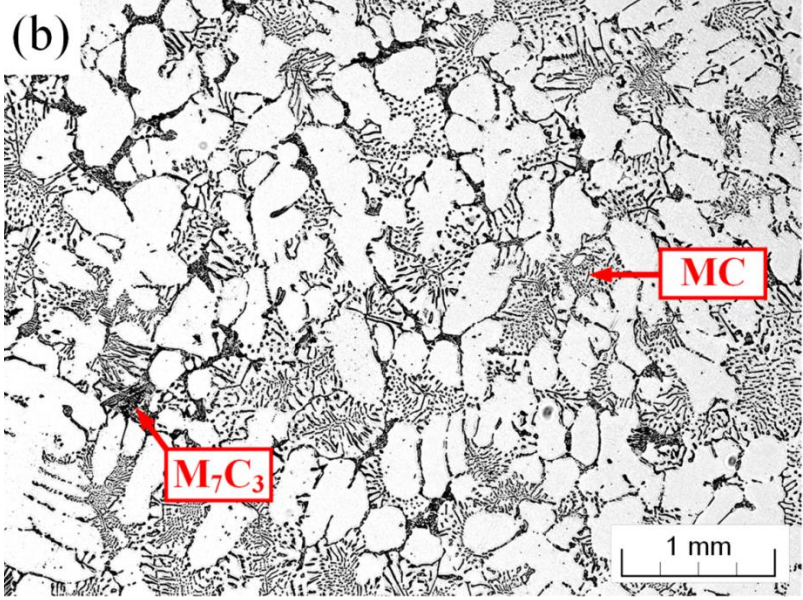
Chapter IV
Experimental Results
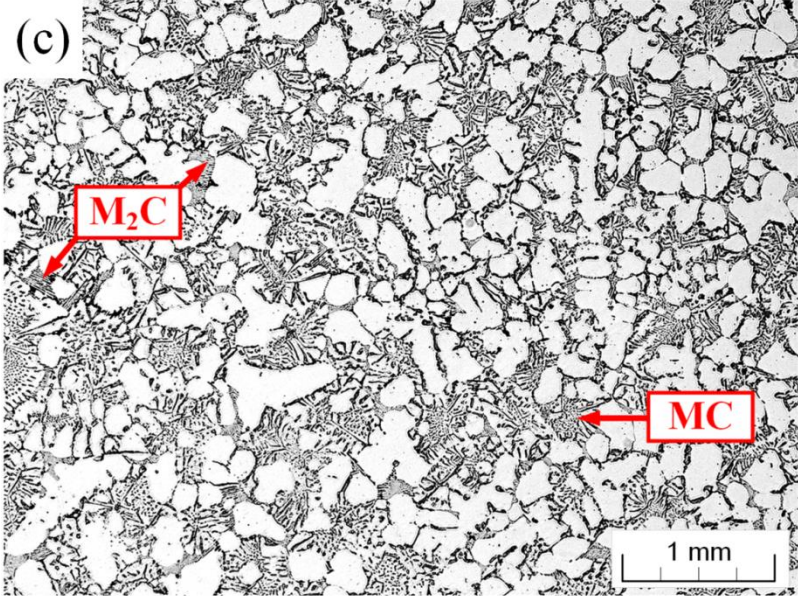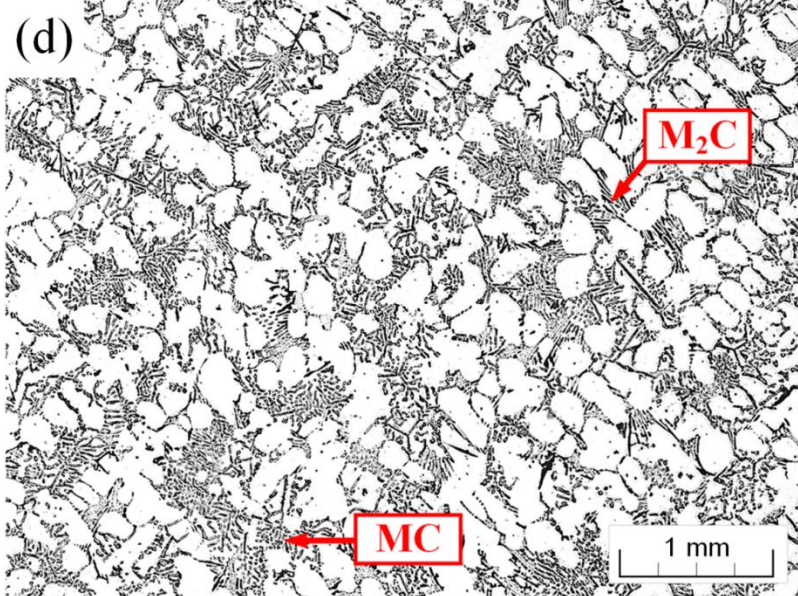
4.1 Microstructure of test specimens in as-cast state

4.1.1 Effect of Mo content on as-cast microstructure

The as-cast specimens varying Mo content were prepared by the metallurgical method and their microstructures were revealed by Nital reagent first and followed by Murakami reagent to observe the microstructure by optical microscope (OM). The results are respectively shown in Fig. 4-1 (a) – (e). It is found that microstructures of all the specimens show hypo eutectic composition consisting of primary austenite dendrite and eutectic structure of (γ + eutectic carbide). The eutectic structures crystallize at the boundary region of primary austenite dendrite, and the types of eutectic carbides precipitating in this series of multi-alloyed white cast irons were MC carbide in string-like or coral-like, M_7C_3 carbide in rod-like or ledeburitic and M_2C carbide in lamellar or plate-like morphologies. The eutectic carbides in 0.12% and 1.17%Mo specimens are MC and M_7C_3 types and those in the specimens with Mo content more than 3% are MC and M_2C types. These results agree well with those by Wu et al [29] that the M_7C_3 carbide precipitated in the multi-alloyed white cast iron with low W_{eq} value (2%Mo + %W), while the M_2C carbide precipitated in the cast iron with high W_{eq} value.

The matrix structure of all specimens is mostly austenite with some martensite. This is because Mo dissolved in the matrix suppresses the pearlite transformation. However, the martensite cannot be distinguished clearly from their microphotographs due to low magnification.

Specimen	Microstructure (by OM)
No. 1 (0.12%Mo)	
No. 2 (1.17%Mo)	

Specimen	Microstructure (by OM)
No. 3 (3.02%Mo)	
No. 4 (4.98%Mo)	

Specimen	Microstructure (by OM)
No. 5 (7.66%Mo)	
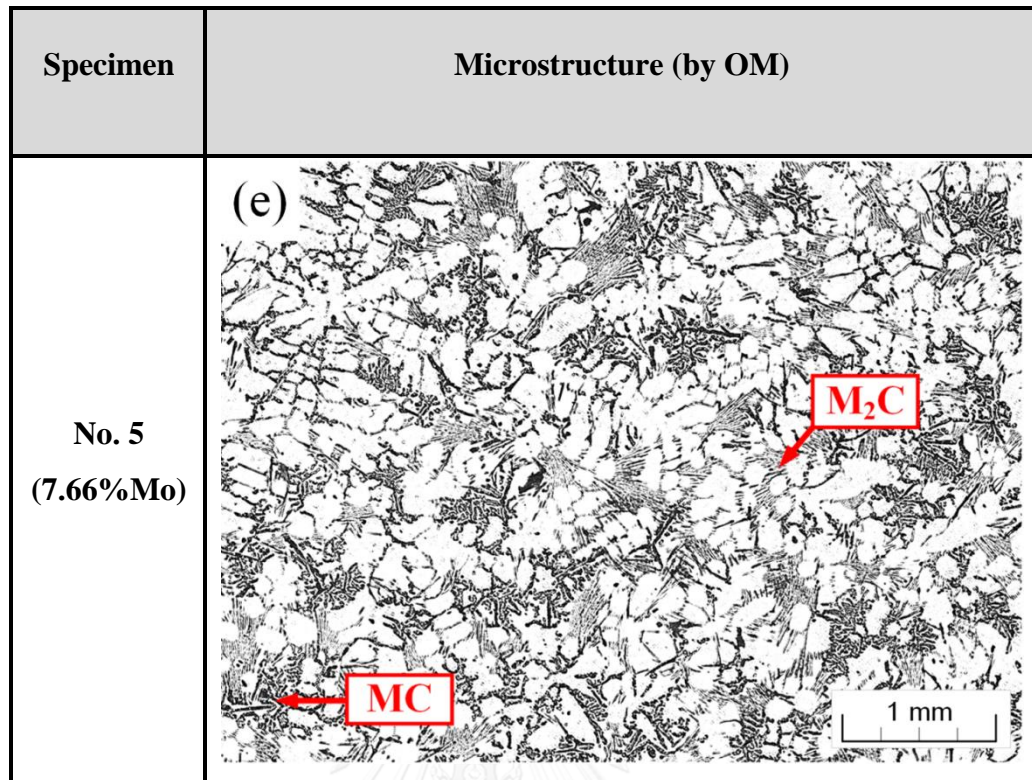
Fig. 4-1 As-cast microstructures of specimens with difference Mo content. (a) 0. 12% Mo, (b) 1. 17% Mo, (c) 3. 02% Mo, (d) 4. 98% Mo and (e) 7.66%Mo specimens. (Etched by Nital and Murakami reagents)

4.1.2 Effect of Mo content on the amount of primary austenite (γ_p) and eutectic structures.

In order to know how Mo addition effected on the volume fraction of phases precipitating from liquid quantitatively, the area fraction (A) of primary austenite dendrite (γ_p) and each type of the eutectic in the as-cast specimens were measured. From the microphotograph, outline of each phase was separated by trace on the tracing paper and the area fraction (A) is measured using an image analysis software. The results are shown in Table 4-1. It is found that the A of primary austenite dendrite changes little in the range of 46.8-48.2%. By contrast, the A of each type of eutectic varies depending on the Mo content. The (γ+MC) eutectic decreases greatly from 43.8% for specimen No. 1 with 0.12%Mo to 24.2% for No. 5 with 7.66%Mo as Mo content of specimen increases. The (γ+M$_2$C) eutectic appears first in the specimen No. 3 with 3.02%Mo, the A of No. 3 is 13.3% and it increases to 28.7% for No. 5 with an increased in Mo content. The A of (γ+M$_7$C$_3$) eutectic changes little in the specimens with 0.12% and 1.17%Mo.

Table 4-1 Area fraction (A) of primary austenite and eutectic structures.

Specimen	Area fraction of primary austenite (%)	Area fraction of eutectic structure (%)		
		γ+MC	γ+M$_7$C$_3$	γ+M$_2$C
No. 1 (0.12%Mo)	46.8	43.8	11.8	
No. 2 (1.17%Mo)	47.1	42.5	10. 6	
No. 3 (3.02%Mo)	46.7	40.8		13.6
No. 4 (4.98%Mo)	48.2	34.0		18.8
No. 5 (7.66%Mo)	47.3	24.2		28.7

4.1.3 Hardness and volume fraction of austenite (Vγ) in as-cast state

Macro- and micro-hardness and volume fraction of austenite (Vγ) in the as-cast specimens are shown in Table 4-2. The hardness of specimen No.1 with 0.12%Mo are 625 HV30 and 597 HV0. 1. In specimen No. 2 with 1. 17%Mo, the hardness are 655 HV30 and 644 HV0. 1, respectively. As for specimen No. 3 with 3. 02%Mo, the hardness obtained are 740 HV30 and 718 HV0. 1. In the specimen No. 4 with 4. 98%Mo, the hardness values are 685 HV30 and 658 HV0. 1. The hardness of specimen No.5 with 7.66%Mo are 643 HV30 and 617 HV0.1. The Vγ values are 32.29, 35.83, 43.84, 34.71 and 23.06% for the specimens with 0.12%, 1.17%, 3.02%, 4.98% and 7.66%Mo, respectively.

Table 4-2 Macro- and micro-hardness and volume fraction of austenite ($V_γ$) in as-cast specimens.

Specimen	Macro-hardness (HV30)	Micro-hardness (HV0.1)	Vγ (%)
No. 1 (0.12%Mo)	625	597	32.29
No. 2 (1.17%Mo)	655	644	35.83
No. 3 (3.02%Mo)	740	718	43.84
No. 4 (4.98%Mo)	685	658	34.71
No. 5 (7.66%Mo)	643	617	23.06

4.2 Effect of Mo content on heat treatment behavior

4.2.1 Effect of Mo content in as-hardened state

4.2.1.1 Hardness and volume fraction of retained austenite (Vγ)

It is known that the macro-hardness is the sum of matrix hardness and eutectic carbides. On the other hand, the micro-hardness is the matrix hardness including the precipitated secondary carbides. The relationship between macro- and micro-hardness and Mo content of specimen are summarized in Table 4-3. The both of macro- and micro-hardness show a similar trend against an increase in the Mo content and they rise with increasing of Mo content. The macro-hardness changed from 882 HV30 for 0.12%Mo to 982 HV30 for 7.66%Mo specimens. The micro-hardness behaves as same as the macro-hardness and it increases from 829 HV0.1 to 935 HV0.1 with an increase in of Mo content. The Vγ decreases greatly from around 40% for 0.12%Mo and 1.17%Mo specimens down to 15% for 7.66%Mo specimen as Mo content increases.

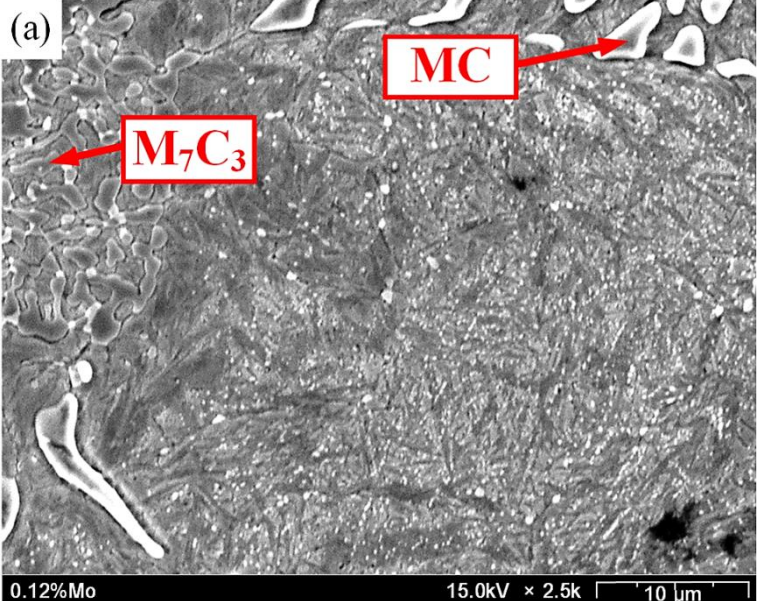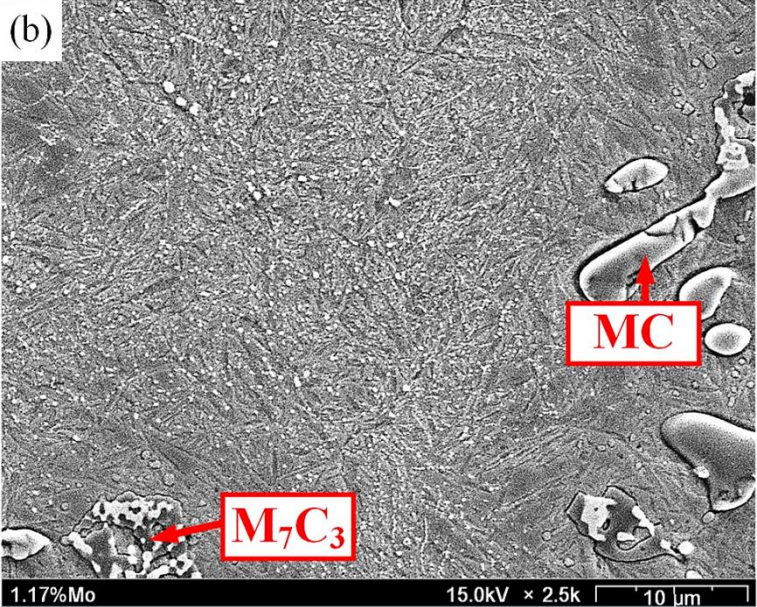**Table 4- 3** Macro- and micro- hardness and volume fraction of austenite (Vγ) in as-hardened specimens with different Mo contents.
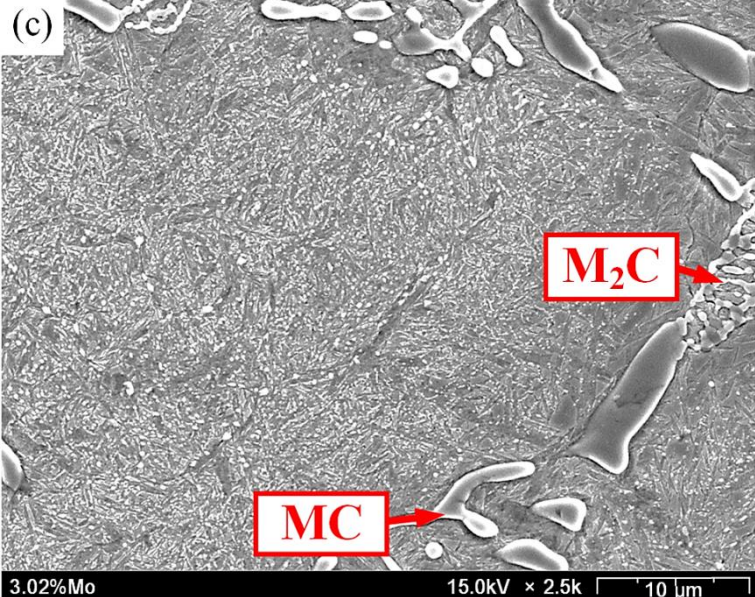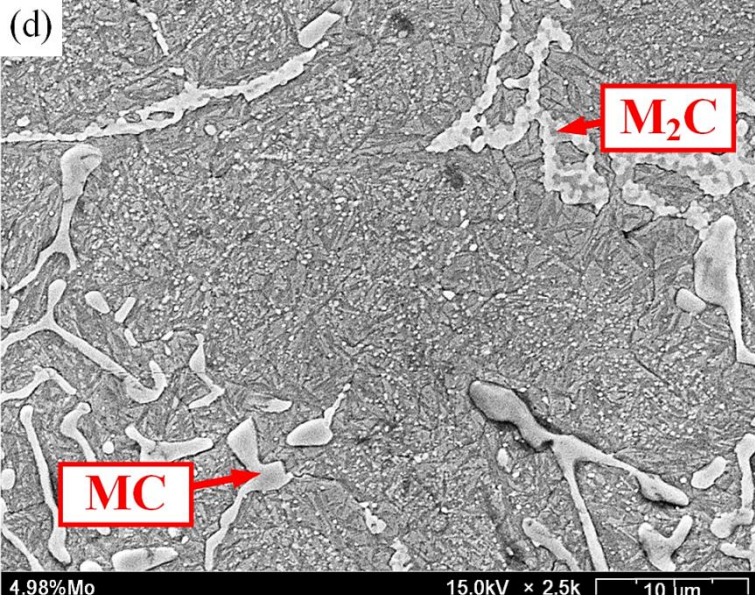
Specimen	Macro-hardness (HV30)	Micro-hardness (HV0.1)	Vγ (%)
No. 1 (0.12%Mo)	882	829	39.09
No. 2 (1.17%Mo)	902	853	40.25
No. 3 (3.02%Mo)	934	884	36.70
No. 4 (4.98%Mo)	941	892	28.05
No. 5 (7.66%Mo)	982	935	14.56

4.2.1.2 Variation of microstructure in matrix

In order to investigate the microstructure of as-hardened specimens, the polished specimens were etched by Villella's reagent and then observed by scanning electron microscope (SME) with focusing on the austenite dendrite. The microstructure in all the as-hardened specimens are shown in Fig. 4-2 (a) – (e). It is well known that the morphology of eutectic carbides changes a little during heat treatment. Paying attention to the matrix microstructure, however, the matrix is composed of fine secondary carbides (Sc), martensite (M) and retained austenite (γ_R). The precipitation of secondary carbides occurs during austenitizing, and they are clearly revealed and seem to increase in number with an increase in Mo content. It was reported that the secondary carbides are mostly MC or M_2C types [7]. The martensite phases transformed from the destabilized austenite can be found all over the matrix but the variation of amount of martensite cannot be clarified from these microphotographs.

From above results, it is clear that the microstructure in as-hardened state is quite different from that in the as-cast state. This demonstrates that the austenite in the as-cast condition is destabilized by the precipitation of fine carbide during austenitizing, and resultantly the unstable austenite transforms into martensite during post cooling.

Specimen	Microstructure (by SEM)
No. 1 (0.12%Mo)	
No. 2 (1.17%Mo)	

Specimen	Microstructure (by SEM)
No. 3 (3.02%Mo)	
No. 4 (4.98%Mo)	

Specimen	Microstructure (by SEM)
No. 5 (7.66%Mo)	
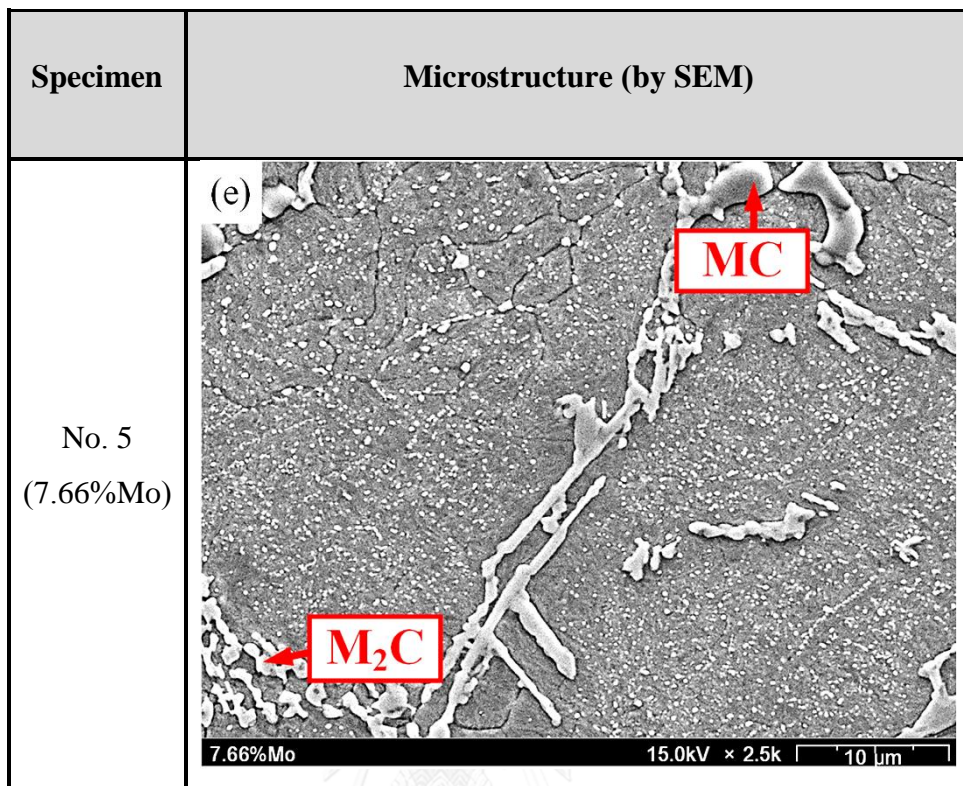
Fig. 4–2 Microstructures of as‑hardened specimens with difference Mo contents.

(a) 0.12%Mo, (b) 1.17%Mo, (c) 3.02%Mo, (d) 4.98%Mo and (e) 7.66%Mo

specimens. (Etched by Villella's reagent)

4.2.2 Effect of Mo content in tempered state

4.2.2.1 Macro-hardness, volume fraction of retained austenite (Vγ) and tempering temperature.

After hardening from austenitizing at 1,373 K for 3.6 ks, the specimens were tempered at several temperatures from 673 to 873 K. The relationship between macro-hardness, Vγ, and tempering temperature are shown in Fig. 4-3 (a) for specimen No. 1 (0.12%Mo), (b) for No. 2 (1.17%Mo), (c) for No. 3 (3.02%Mo), (d) for No. 4 (4.98%Mo) and (e) for No. 5 (7.66%Mo), respectively. The data of hardness and Vγ values in as-hardened state were plotted in each figure for better understanding of the tempering behavior.

In each tempering curve, the hardness drops greatly from that in as-hardened state when the specimen is tempered at 673K. After that, the hardness begins to rise to the maximum point, and subsequently, it lowers over a certain tempering temperature. In other words, the tempered hardness curve shows an evident secondary hardening. It is believed that this variation of hardness is related to the phase transformation of matrix. The increase of hardness is due to the precipitation of secondary carbides from austenite during tempering and the rest of austenite transforms to martensite during post cooling. Additionally, a decrease in the amount of austenite is one reason. The mutual relations between the increasing of martensite and the decreasing of retained austenite (γ_R), as well as the precipitation of secondary carbides, determine the matrix hardness.

In the specimen No. 1 with 0.12%Mo as shown in Fig. 4-3 (a), the hardness drops sharply when the specimen is tempered at 673 K. As tempering temperature increases, subsequently, the hardness continues to rise gradually, until the maximum hardness is obtained at 798 K. When it is tempered over 798 K, the hardness decreased

greatly due to over tempering. Here, the degree of secondary hardening (ΔHs) is defined as the difference in hardness between the maximum tempered hardness (H_{Tmax}) and the hardness at which the degree of secondary hardening begins. The H_{Tmax} of 855 HV30 was obtained at 798 K tempering and the ΔHs is 98 HV30. With respect to the austenite, around 40%$V\gamma$ existed in as-hardened state decreases gradually as the tempering temperature rises and then it gets to about 4% at 873 K tempering. The $V\gamma$ value at the H_{Tmax} is 8%.
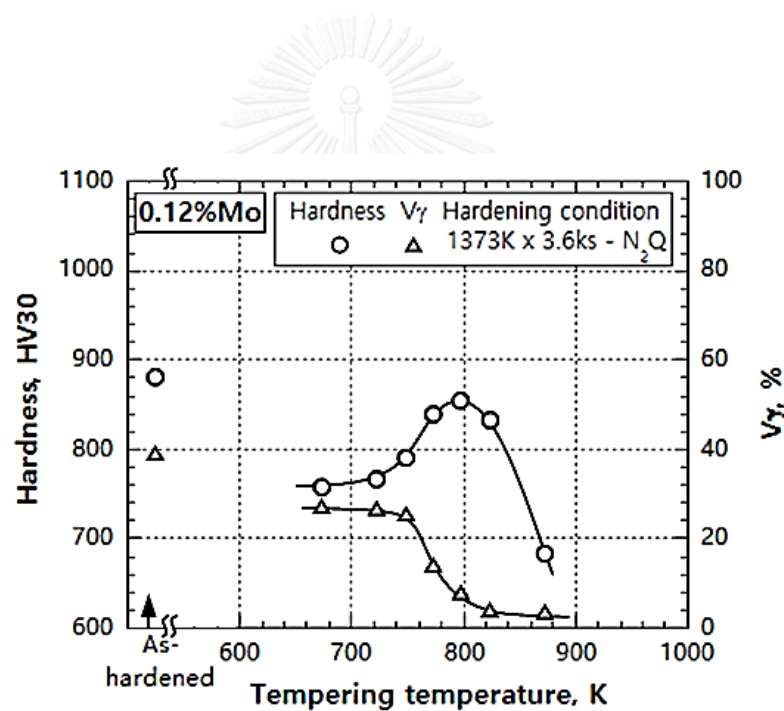
Fig 4-3. (a) Relationship between macro-hardness, $V\gamma$ and tempering temperature of specimen No. 1 (0.12%Mo)

In the case of specimen No. 2 with 1.17%Mo in Fig. 4-3 (b), the tempered hardness curve shows similar behavior to that in specimen No. 1. The hardness in as-hardened state decreases greatly in tempering at 673 K and it also shows the secondary hardening with the H_{Tmax} of 886 HV30 obtained at 798 K tempering. Then, ΔHs is 99 HV30. The $V\gamma$ in as-hardened state was about 40% and it almost the same as the case of specimen No. 1. The $V\gamma$ gradually reduces with an increase in the tempering temperature and finally, the $V\gamma$ of 3% was left at 873 K temping. The $V\gamma$ at the H_{Tmax} is 10%.
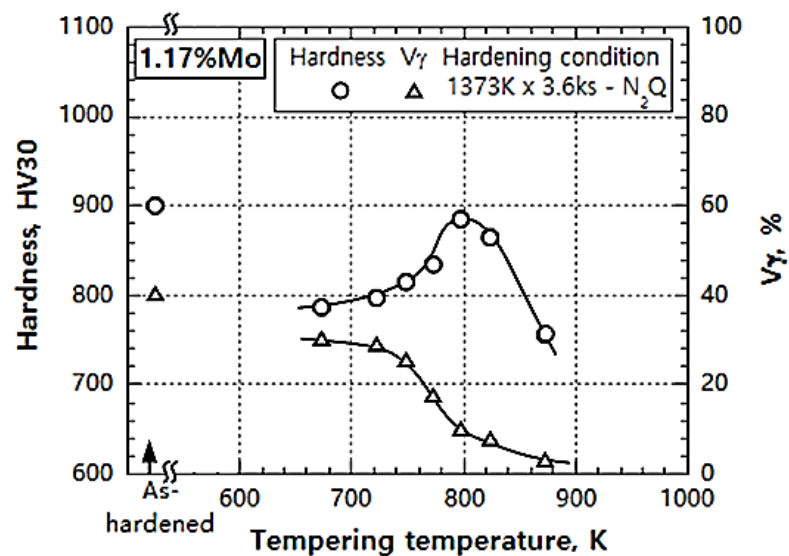
Fig 4-3. (b) Relationship between macro-hardness, $V\gamma$ and tempering temperature of specimen No. 2 (1.17%Mo)

The tempered hardness curve of specimen No. 3 with 3.02%Mo is shown in Fig. 4-3 (c). The tempered hardness curve shows a tendency similar to those of specimen No. 1 and No. 2. The hardness increases gradually as the tempering temperature rises to the H_{Tmax} of 913 HV30 at 798 K tempering. Over 798 K, it decreases remarkably. The ΔHs is 109 HV30 and the 37% $V\gamma$ in as-hardened state decreases greatly by the tempering and decreases to 3% $V\gamma$ at 873 K. The $V\gamma$ at the H_{Tmax} is 8%.

Fig. 4-3 (c) Relationship between macro-hardness, $V\gamma$ and tempering temperature of specimen No. 3 (3.02%Mo)

Fig. 4-3 (d) shows the tempered hardness curve and the change in Vγ of specimen No. 4 with 4.98%Mo. The hardness curve shows similar behavior to those of the specimen No. 1, No. 2 and No. 3. The hardness in each tempering is the highest in the four specimens. The tempered hardness increases to the H_{Tmax} of 948 HV30 at 798 K. The ΔHs is 115 HV30. The Vγ in tempered state begins to reduce abruptly over the tempering temperature of 748 K and that at 873 K tempering is 2%. The Vγ at H_{Tmax} is 6%.
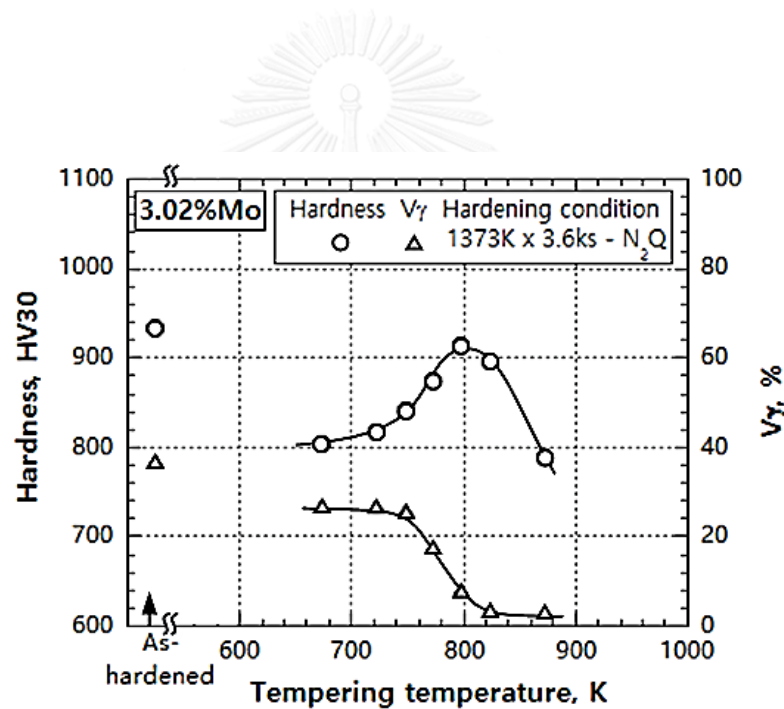
Fig. 4-3 (d) Relationship between macro-hardness, Vγ and tempering temperature of specimen No. 4 (4.98%Mo)

In the case of the specimen No.5 with highest Mo content of 7.66%Mo is shown in Fig. 4-3 (e). The tempered hardness curve shows roughly similar behavior to those of the other specimens in the group. However, the increasing rate of hardness before arriving at H_{Tmax} is small and not sharp compared with others. The H_{Tmax} of 916 HV30 was obtained at 798 K tempering. The ΔHs of 50 HV30 is lowest. The relation of $V\gamma$ vs. tempering temperature shows good correspondence to that of the hardness vs. tempering temperature; As the $V\gamma$ lowers, the hardness rises. The $V\gamma$ of 15% in as-hardened state begins to drop from the tempering temperature of 773 K tempering with an increase in the tempering temperature. On the other side, the retained austenite (γ_R) disappears when the specimen is tempered at 873K. The $V\gamma$ value at the H_{Tmax} is about 2%.

In all the specimens described above, the reason why the hardness decreases remarkably by tempering over the temperature at the H_{Tmax} is mainly due to the coarsening of precipitated secondary carbides.
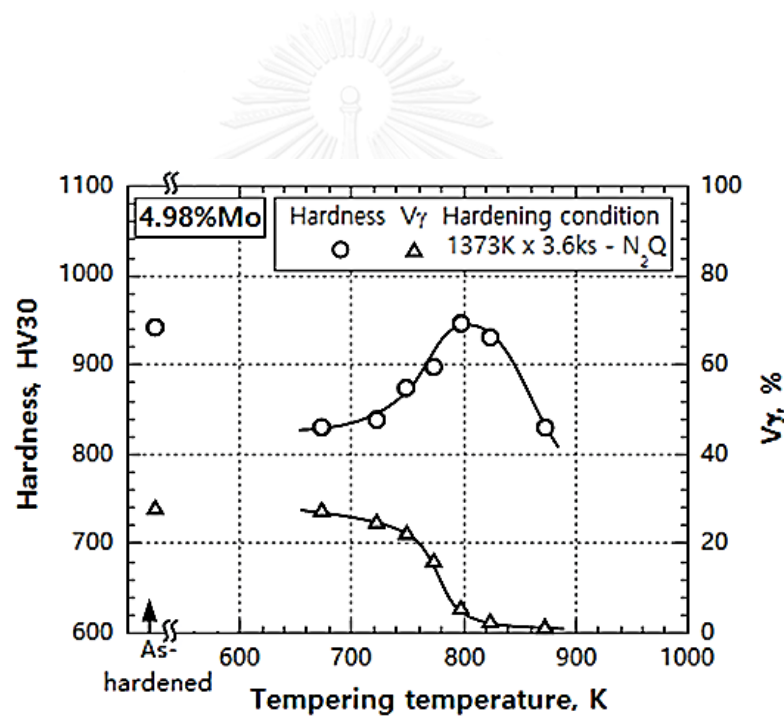

Fig 4-3 (e) Relationship between macro-hardness, $V\gamma$ and tempering temperature of specimen No. 5 (7.66%Mo)

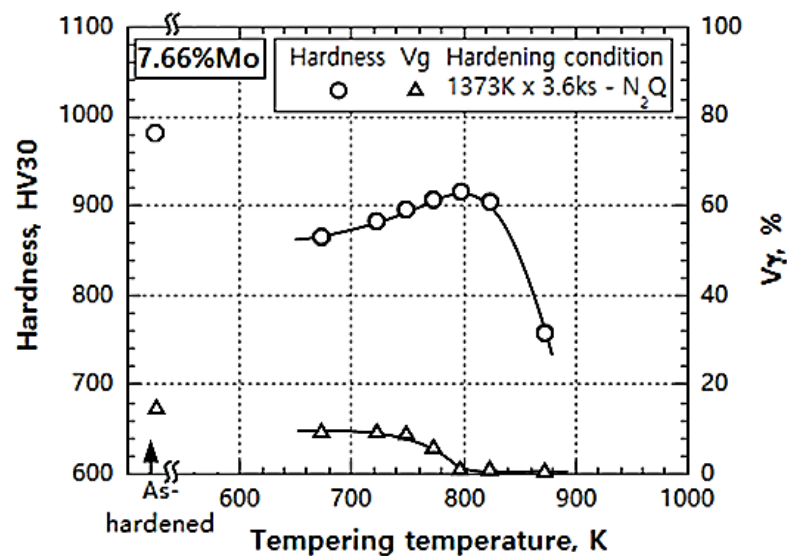*4. 2. 2. 2 Micro- hardness, volume fraction of retained austenite (Vγ) and tempering temperature.*

The hardness of matrix can be widely varied by heat treatment and it controls the mechanical properties of cast alloy including wear resistance. Therefore, it is valuable to measure the micro-hardness of matrix relating to the condition of heat treatment. The relationship between micro- hardness, volume fraction of retained austenite (Vγ) and tempering temperature are shown in Fig. 4-4 (a), (b), (c), (d) and (e) for each specimen.

According to the figures, it can be seen that the curves of tempered hardness adopting the micro- hardness show very similar trend to those constructed by macro- hardness. Even in specimen No. 5 with highest Mo content of 7. 66%, the secondary hardening appears clearly. In every specimen, the micro-hardness lies at lower position than the macro- hardness. This proves that in macro- hardness, the hardness of the eutectic carbide is added to the matrix hardness. Therefore, the secondary precipitation hardening in the matrix makes the H_{Tmax} show outstanding on the tempered hardness curve compared with those by macro-hardness.

The ΔHs values are 112 HV0.1 for specimen No. 1, 118 HV0.1 for No. 2, 123 HV0.1 for No. 3, 149 HV0.1 for No. 4 and 71 HV0.1 for No. 5, respectively. From micro-hardness curves, the H_{Tmax} values were 808 HV0.1 for specimen No. 1, 843 HV0.1 for No. 2, 884 HV0.1 for No. 3, 905 HV0.1 for No. 4 and 889 HV0.1 for No. 5, respectively.

The tempering temperatures at which the H_{Tmax} of micro-hardness is obtained agree exactly with those obtained by macro- hardness. From all the results, it can be said that the variation of macro-hardness is little affected by eutectic carbides

but based on that of the micro-hardness. Therefore, it is not problem to discuss the heat treatment behavior of matrix by using macro-hardness.
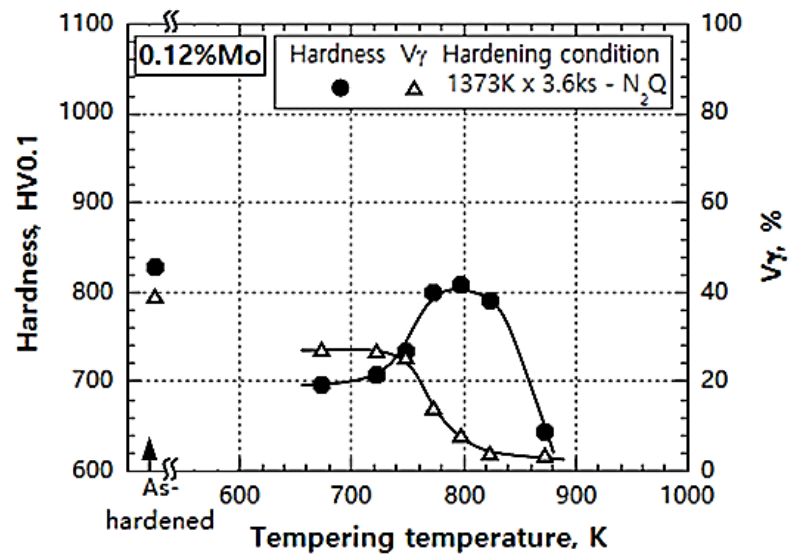
(a) Specimen No. 1 (0.12%Mo)
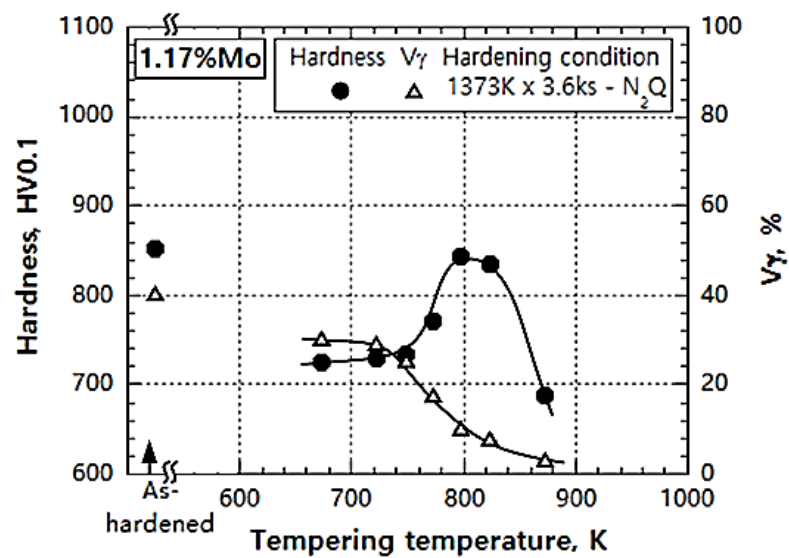
(b) Specimen No. 2 (1.17%Mo)
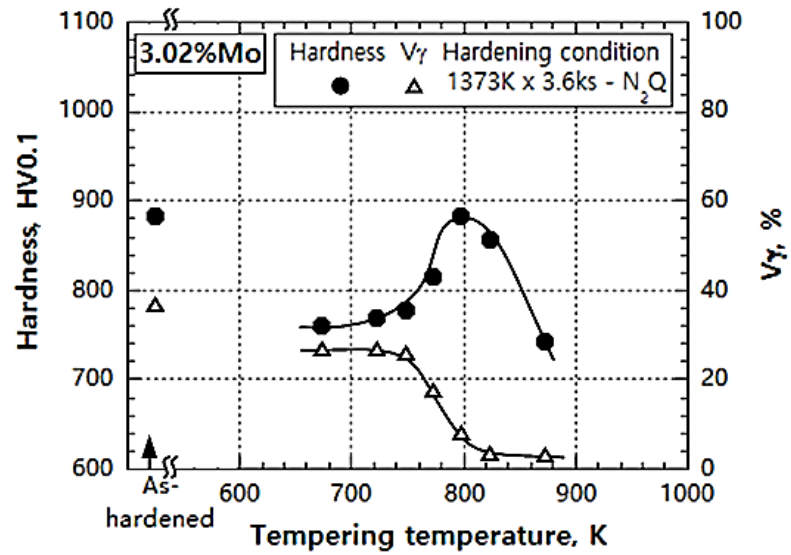
(c) Specimen No. 3 (3.02%Mo)
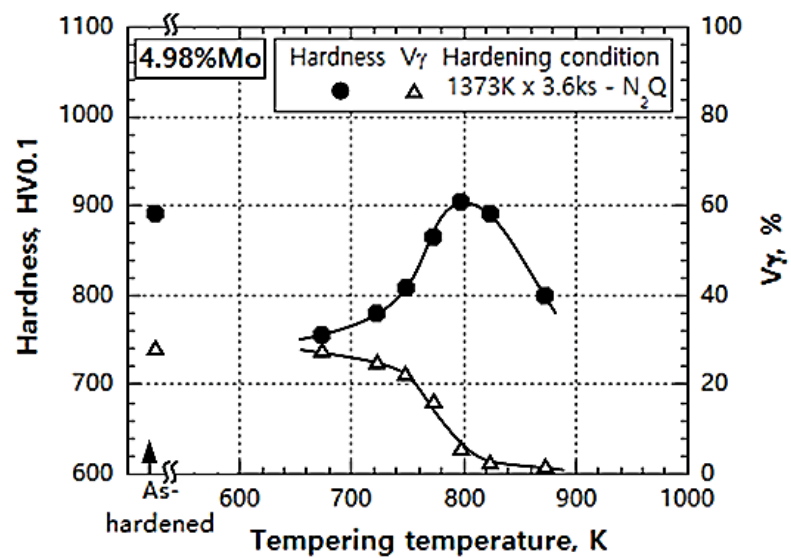
(d) Specimen No. 4 (4.98%Mo)
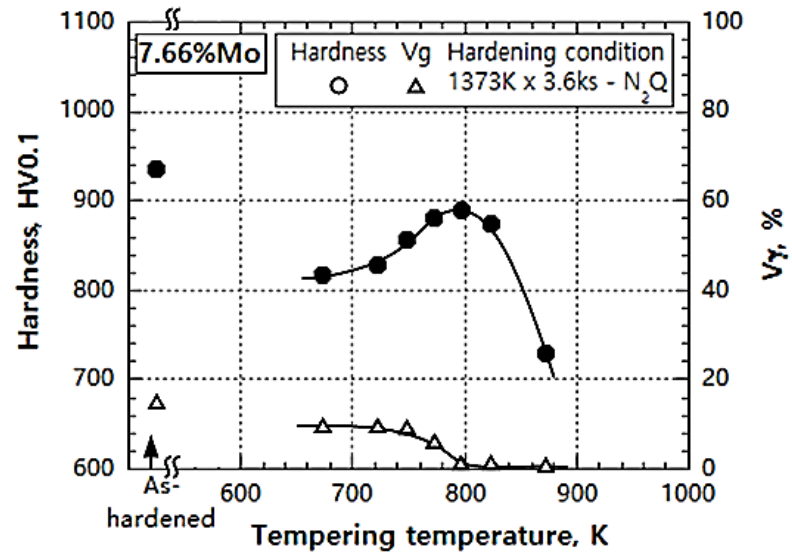
(e) Specimen No.5 (7.66%Mo)

Fig. 4-4 Relationship between micro-hardness, volume fraction of retained austenite

(Vγ) and tempering temperature. (a) 0.12%Mo, (b) 1.17%Mo, (c) 3.02%Mo,

(d) 4.98%Mo and (e)7.66%Mo specimens.

Chapter V

Discussions

5.1 As-cast microstructure of test specimens varying Mo content

5.1.1 Effect of Mo content on variation of microstructure

In order to understand solidification sequence from as-cast microstructure, thermal analysis is generally introduced. As an example, thermal analysis of 7.66%Mo specimen was carried out and the analysis curve is shown in Fig. 5-1. It is found that solidification sequence starts with precipitation of primary austenite (γ_p) from the melt, followed by eutectic reaction of $L \rightarrow (\gamma+MC)_E$ and that of $L \rightarrow (\gamma+M_2C)_E$, continuously. This result agrees well with the research by Wu et al [21]. To determine the temperature of each solidification accurately, the first deviation of the curve (dT/dt) was obtained by adopting the points of temperature and time about 1,200 on the curve. The first deviation curve shows the peaks of freezing points for some phases. The first peak in Fig. 5-1 is considered to be the precipitation of primary austenite dendrite (γ_p), followed by the reactions of ($\gamma+MC$) eutectic and ($\gamma+M_2C$) eutectic, respectively.

Comparing the deviation graph with the thermal analysis curve as shown in Fig. 5-1, the temperatures for the phases to solidify can be determined and it is summarized as follows.

The first peak is primary austenite dendrite and it is expressed by,

$$L \rightarrow \gamma_p \qquad \text{at 1,574K}$$

The second recalescence in the curve is considered to be the following eutectic reaction,

$$L \rightarrow (\gamma+MC)_E \qquad \text{at 1,557K}$$

Then, the last one represents another eutectic reaction,

$$L \rightarrow (\gamma + M_2C)_E \qquad\qquad \text{at } 1,502K$$
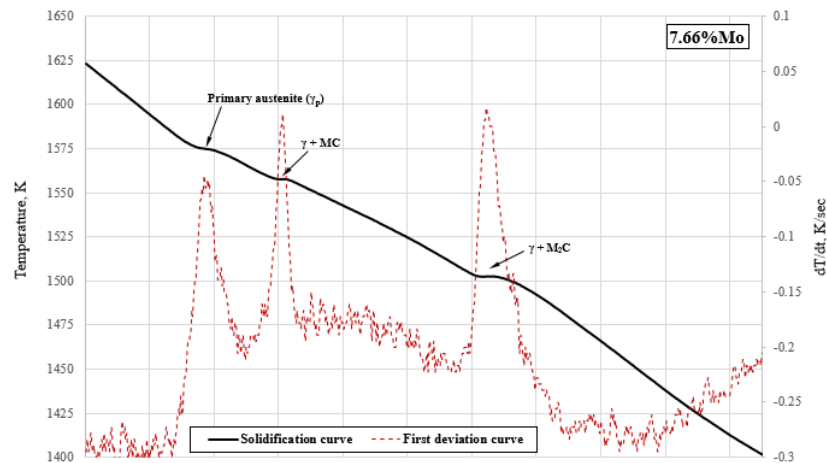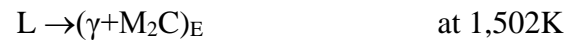
Fig. 5-1 Comparison of thermal analysis curve and first deviation graph of specimen

No. 5 with 7.66% Mo.
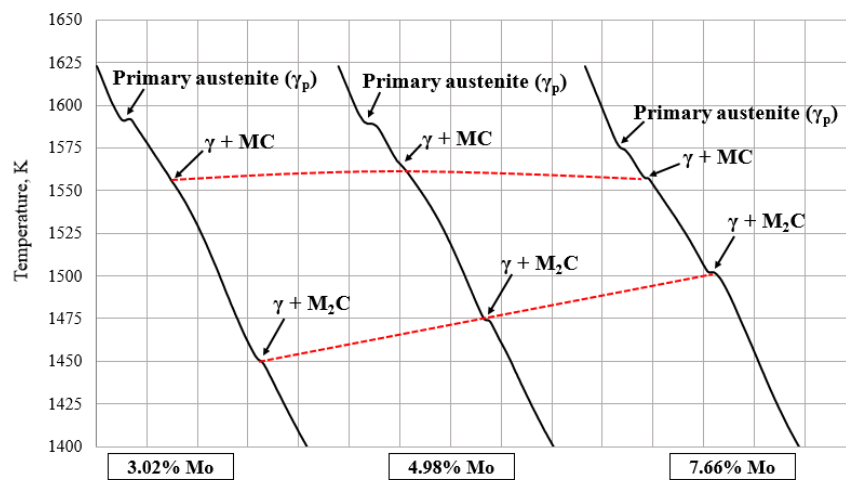
Fig. 5-2 The solidification curves of specimens with different Mo contents.

The solidification curves of specimens with 3.02, 4.98 and 7.66%Mo are respectively shown in Fig. 5-2. It is found that the three recalescence points on the curves of specimen with 3.02 and 4.98%Mo are very similar to that of the specimen with 7.66%Mo shown in Fig. 5-1. However, the temperatures at the recalescence are remarkably different. The solidification sequence of 3.02%Mo specimen is represented by the reactions show by the next formulas,

$$L \rightarrow \gamma_p \qquad \text{at } 1,592\text{K}$$

$$L \rightarrow (\gamma+MC)_E \qquad \text{at } 1,557\text{K}$$

$$L \rightarrow (\gamma+M_2C)_E \qquad \text{at } 1,450\text{K}$$

As for the specimen with 4.98%Mo, the solidification sequence is shown by the following reactions.

$$L \rightarrow \gamma_p \qquad \text{at } 1,589\text{K}$$

$$L \rightarrow (\gamma+MC)_E \qquad \text{at } 1,565\text{K}$$

$$L \rightarrow (\gamma+M_2C)_E \qquad \text{at } 1,473\text{K}$$

The relationship between start of solidifying temperature of primary austenite (γ_p), eutectic reactions and Mo content is shown in Fig. 5-3. It can be seen that the start of solidifying temperature of primary austenite decreases a little from 1,575 to 1,600K as the Mo content increases. As for the freezing temperature of the ($\gamma+MC$) eutectic, it seems not to change. In the case of the ($\gamma+M_2C$) eutectic reaction, by contrast, it increases gradually with an increase in Mo content ranging from 1,450 to 1,500K. When the solidification range of ($\gamma+MC$) eutectic is considered, it decreases clearly with increasing the Mo content.
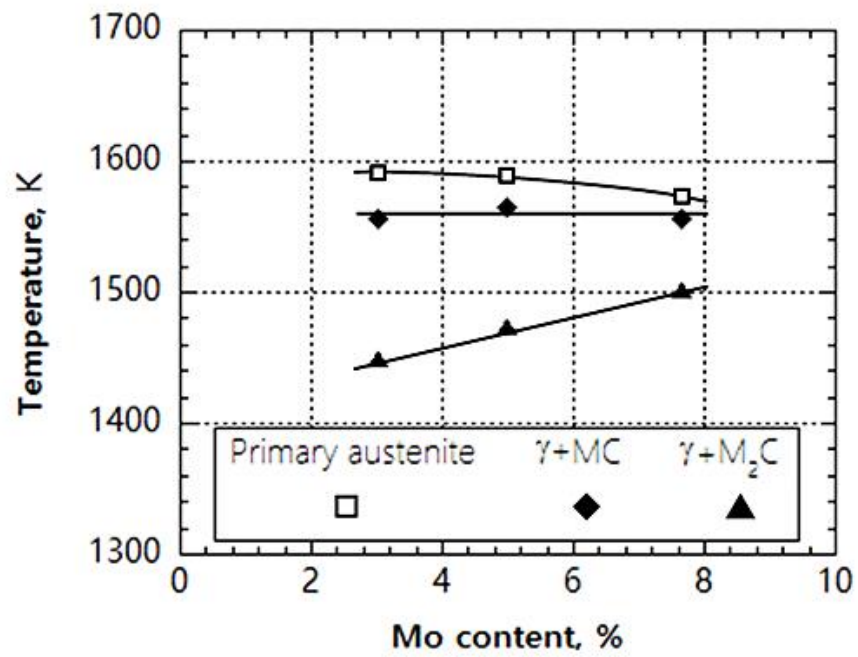
Fig. 5-3 Relationship between start of solidifying temperature of primary austenite (γ_p),

(γ+MC) eutectic, (γ+M$_2$C) eutectic and Mo content.

It is profitable to know the change of constituent of each phase in the microstructure by the addition of Mo. The area fraction of each phase in the as-cast microstructure was measured using an image analyzer and the result is shown in Fig. 5-4. The area fraction of primary austenite and total of eutectic structures do not change, the area fraction of primary austenite and total eutectic carbide are about 47% and 53%, respectively, even if Mo content increases. However, the area fraction of eutectic structure varies greatly depending on the Mo content. The $(\gamma+M_7C_3)$ eutectic which appears in the specimen with very low Mo content decreases with an increase in Mo content and disappears at Mo content over 1.17%. Instead of it, $(\gamma+M_2C)$ eutectic appears at Mo% more than 3.02% and increases in proportion to Mo content. On the other hand, the area fraction of $(\gamma+MC)$ eutectic decreases progressively as the Mo content increases. These results show in good accordance with those of thermal analysis curves show in Fig. 5-2. It can be explained that the solidification temperature range of $(\gamma+MC)$ eutectic decreases by an increase of solidification temperature range of $(\gamma+M_2C)$ eutectic with increasing the Mo content. Therefore, it can be understood that the solidification of $(\gamma+M_2C)$ eutectic affects that of $(\gamma+MC)$ eutectic. This is because an increase in Mo content promotes the $(\gamma+M_2C)$ eutectic significantly.
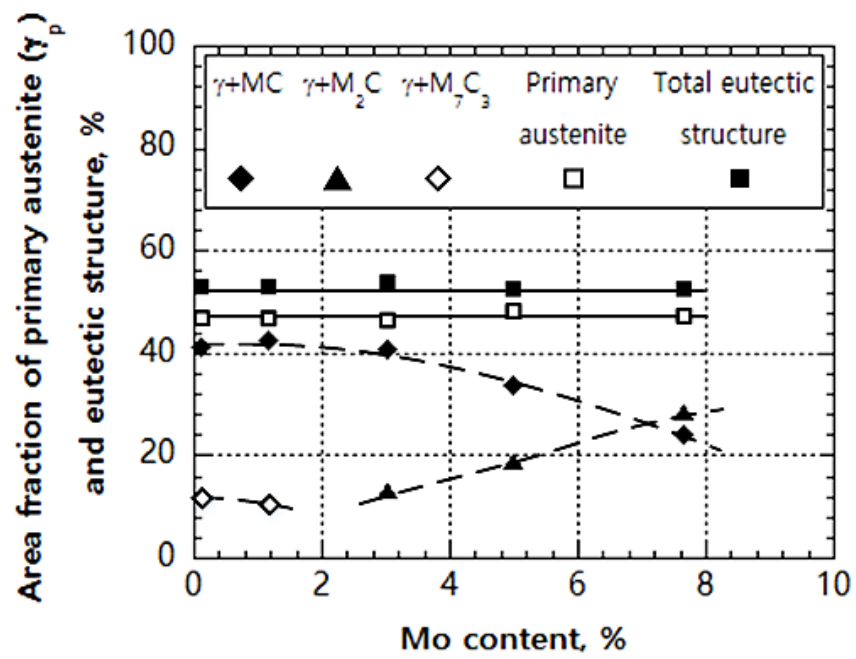
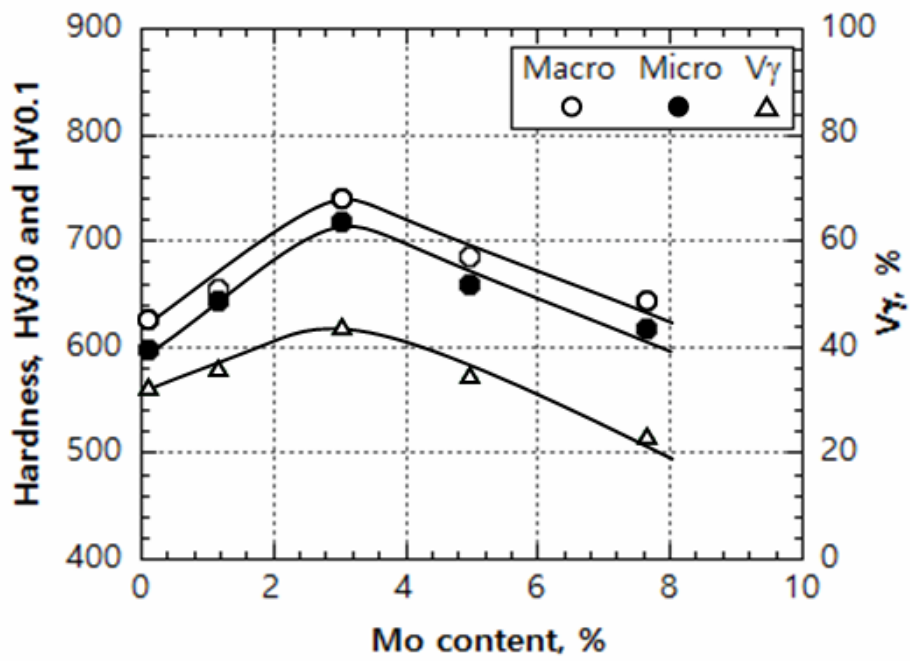**Fig. 5-4** Relationship between area fraction of primary austenite (γ_p), eutectic structures

and Mo content.

5.1.2 Effect of Mo content on hardness and volume fraction of retained austenite (Vγ) in as-cast state

It is known that the macro-hardness is sum of the hardness of matrix and eutectic structure. On the other side, the micro-hardness is the hardness of matrix only. The effect of Mo content on macro- and micro-hardness and V_γ value in the as-cast state is shown in Fig. 5-5 for all of specimens. The macro- and micro-hardness increase gradually to the maximum value as Mo content increases to 3.02%. After that, they decrease as the Mo content increases. The increasing of hardness in the former state should be due to a rise of amount of M_2C eutectic carbide which has higher hardness than M_7C_3 eutectic carbide as well as a decrease in amount of M_7C_3. The decreasing of hardness in the later stage over 3.02%Mo is considered because of a decrease in the amount of MC eutectic carbide which has higher hardness than M_2C carbide.

The V_γ in the as-cast iron increases in the former state and decreases in the later stage with an increase in the Mo content. An increase in the V_γ is due to the fact that an increasing of Mo content in austenite lower the Ms temperature. The highest V_γ value of 43.84% is obtained in the specimen with 3.02%Mo. On the other side, a decrease of the V_γ in specimens with more than 3%Mo is caused by the reason that more C and Mo consumed to form M_2C eutectic carbides at the end of solidification. In other words, the reduction of C and Mo contents in austenite solidified make the Ms temperature rise and then, more martensite exists.
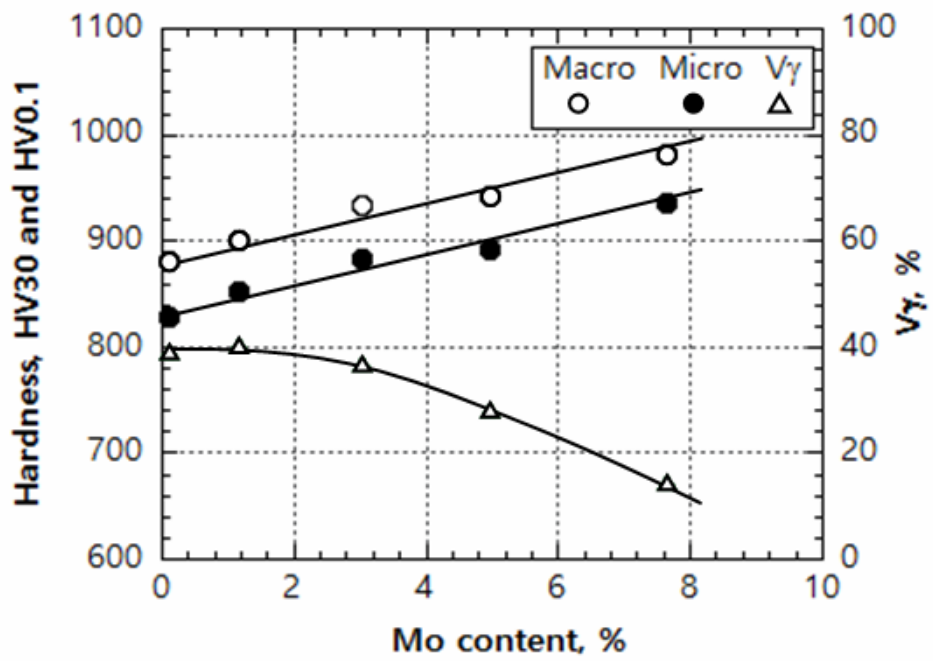
Fig. 5-5 Relationship between macro- and micro-hardness, volume fraction of retained

austenite (Vγ) and Mo content in as-cast irons.

5.2 Effect of Mo content on hardness and volume fraction of retained austenite (Vγ) in as-hardened state

It is believed that the eutectic carbides change little during heat treatment. Therefore, the variation of hardness by heat treatment depends on the phase transformation of matrix, i.e. the micro-hardness. The relationship between macro- and micro-hardness, Vγ value and Mo content in as-hardened state is shown in Fig. 5-6. The macro-hardness increases progressively as the Mo content increases. The micro-hardness shows similar behavior to the macro-hardness. The reason for an increase in hardness is due to an increase in a number of eutectic M_2C carbides with high hardness and the precipitation of special secondary carbides together with more martensite in the matrix. It is found from Fig. 5-6 that the micro-hardness locates overall at lower position than the macro-hardness. This is because the macro-hardness expressed by the total hardness of eutectic carbide and matrix.

The Vγ continues to decrease with raising the Mo content. This suggests that the amount of martensite is increased together with the more precipitated secondary carbides. The precipitation of secondary carbides results in reduction of C and alloying elements in austenite. Subsequently, the Ms temperature is raised and Vγ is down.

**Fig. 5-6** Relationship between macro- and micro-hardness, volume fraction of retained

austenite (Vγ) and Mo content in as-hardened state.

5.3 Effect of Mo content on microstructure, hardness and volume fraction of retained austenite (Vγ) in tempered state

**5.3.1 Variation of matrix microstructure in tempered specimens**

Matrix hardness or micro-hardness of multi-alloyed white cast iron is closely related to the transformation behavior of matrix. In order to discuss the change in the microstructure by tempering, as-hardened and transformed microstructures of specimens with greatly difference in Mo content was investigated in detail by using SEM. The microstructures of as-hardened specimen is shown in Fig. 5-7 (a) and those of tempered specimens of which hardness are lower than H_{Tmax}, H_{Tmax} and higher than H_{Tmax} are shown in Fig. 5-7 (b), (c) and (d) for specimen No. 2 with 1.17%Mo. The microstructure of specimen No. 5 with 7.66%Mo takes by the same condition as specimen No. 2 is shown in Fig. 5-7 (a) - (d).

In the Fig. 5-7 (a), as-hardened specimen with 1.17%Mo has a large amount of austenite coexisting with martensite and secondary carbides in matrix. There exist some secondary carbides in large size in some matrices. They could be indissoluble carbides precipitated previously during annealed. In the matrix of test piece tempered at 723K that is a temperature lower than H_{Tmax}, the amount of retained austenite does not so different from the as-hardened specimen. However, the newly precipitated fine carbides are observed. When the tempering temperature is increased to 798K at which H_{Tmax} was obtained, much more fine carbides can be seen as well as the secondary carbides are increased. On the other side, the retained austenite is decreased while the martensite is increased.
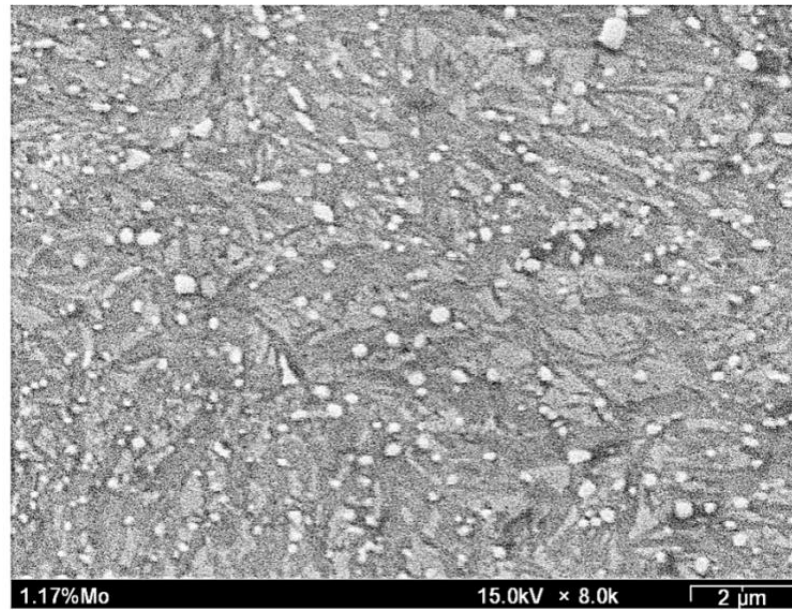
(a) As-hardened

(Hardness: 902 HV30 and 853 HV0.1, Vγ: 40.24%)
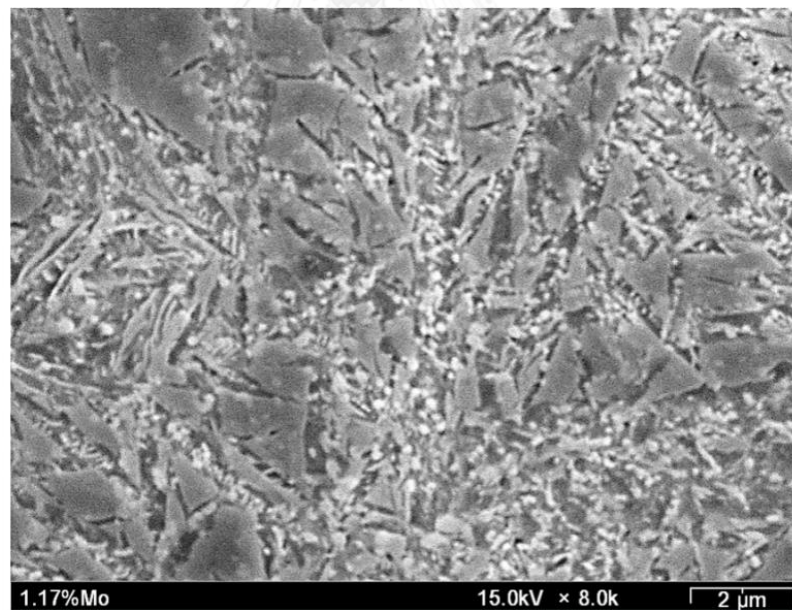
(b) Tempered at 723K

(Hardness: 797 HV30 and 729 HV0.1, Vγ: 28.78%)
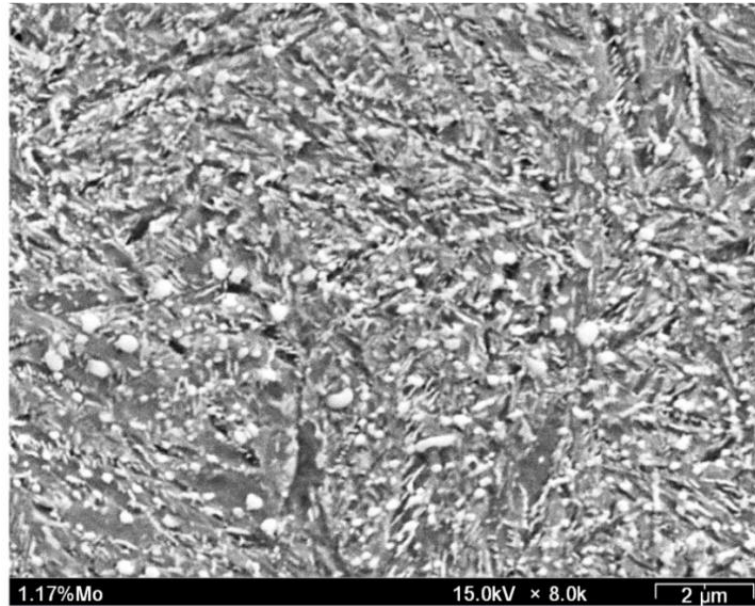
(c) Tempered at 798K

(Hardness: 886 HV30 and 843 HV0.1, Vγ: 10.05%)
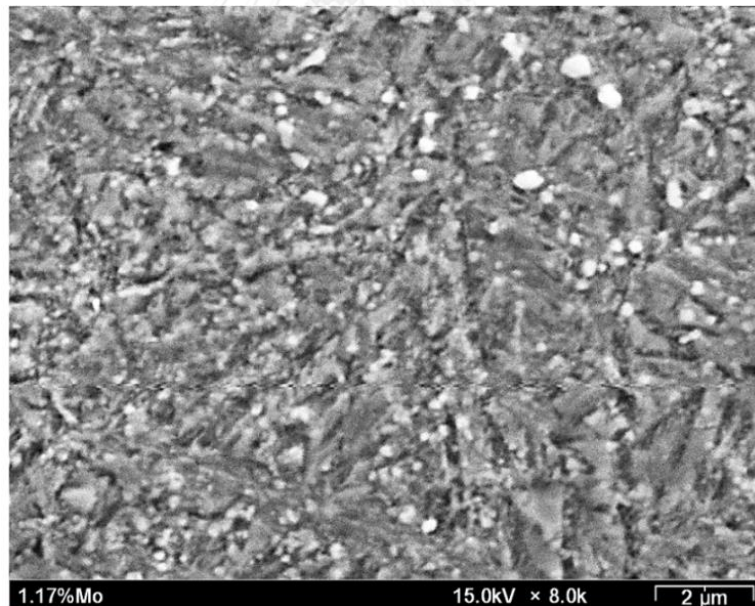
(d) Tempered at 873K

(Hardness: 756HV30 and 688HV0.1, Vγ: 3.15%)

Fig. 5-7 SEM micrographs of specimen No.2 with 1.17%Mo. (a) As-hardened from 1,373K, (b) Tempered at 723K (lower than H$_{Tmax}$), (c) Tempered at 798K (H$_{Tmax}$) and (d) Tempered at 873K (higher than H$_{Tmax}$).

It is reported that the precipitated secondary carbides are MC, M_2C M_6C or $M_{23}C_6$ types which depend on the chemical composition of the cast iron [7]. The secondary carbides are found in granular morphology. At 873K tempering, on the other hand, the secondary carbides lower in amount but enlarge in size. In this point, either martensite or retained austenite cannot be distinguished. Under this tempering condition, the coarsening of carbides by over-tempering occurred. It is believed that the over-tempering suppresses the secondary hardening greatly.

The results of specimen with 7.66% Mo are shown in Fig. 5-8 (a) − (d), as-hardened matrix structure consists of secondary carbides in large massed shape and martensite and retained austenite can be seen clearly. The distribution of secondary carbides is similar to that of specimen with 1.17% Mo. However, the amount of retained austenite is much smaller and the size of secondary carbides is relatively larger. It is clear that many carbides in small size precipitate secondarily by tempering at 723K, as well as the retained austenite is decreased. The precipitation continues at 798K tempering by which the H_{Tmax} is obtained. When tempering temperature is elevated to 823K, the coarsening of the fine carbide takes place and most of fine carbides disappear.

By comparing the micro-hardness of H_{Tmax} for the 1.17% Mo specimen with that for 7.66% Mo, it is found that the micro-hardness of 7.66%Mo specimen is higher than that of 1.17%Mo specimen. The reason is mainly due to the difference in the kind and amount of precipitated secondary carbides but the amount of martensite can be one reason. Therefore, it can be said that an increase in Mo content contributed more to increase the precipitation of secondary carbides and the martensite transformations from retained austenite during tempering except for the case of over-tempering.
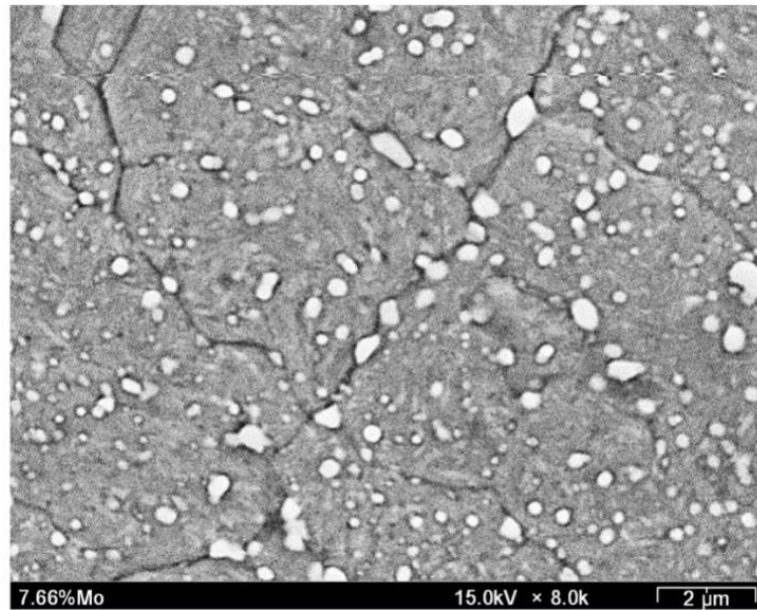
(a) As-hardened

(Hardness: 982 HV30 and 935 HV0.1, Vγ: 14.56%)
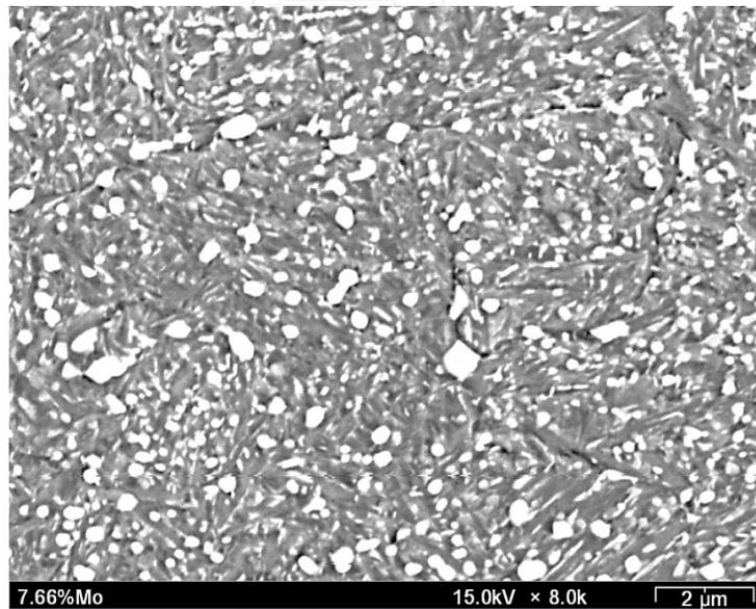
(b) Specimen tempered at 723K

(Hardness: 883 HV30 and 828 HV0.1, Vγ: 9.55%)
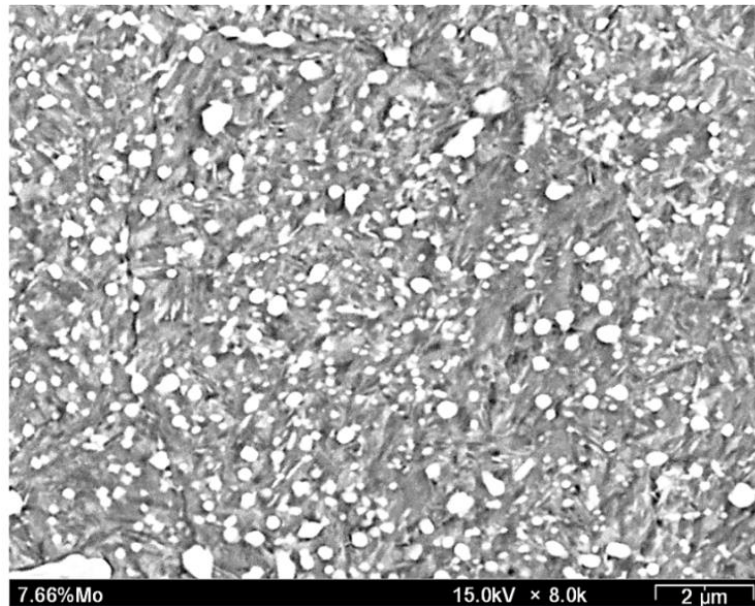
(c) Tempered at 798K

(Hardness: 916 HV30 and 889 HV0.1, $V\gamma$: 1.50%)
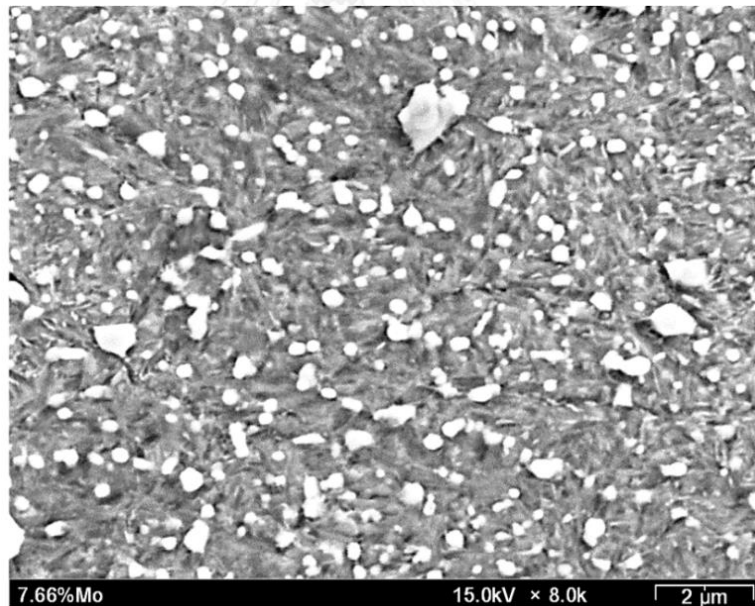
(d) Tempered at 873K

(Hardness: 7589HV30 and 729HV0.1, $V\gamma$: 1.09%)

Fig. 5-8 SEM micrographs of specimen No. 5 with 7.66%Mo. (a) As-hardened from 1,373K, (b) Tempered at 723K (lower than H_{Tmax}), (c) Tempered at 798K (H_{Tmax}) and (d) Tempered at 873K (higher than H_{Tmax}).
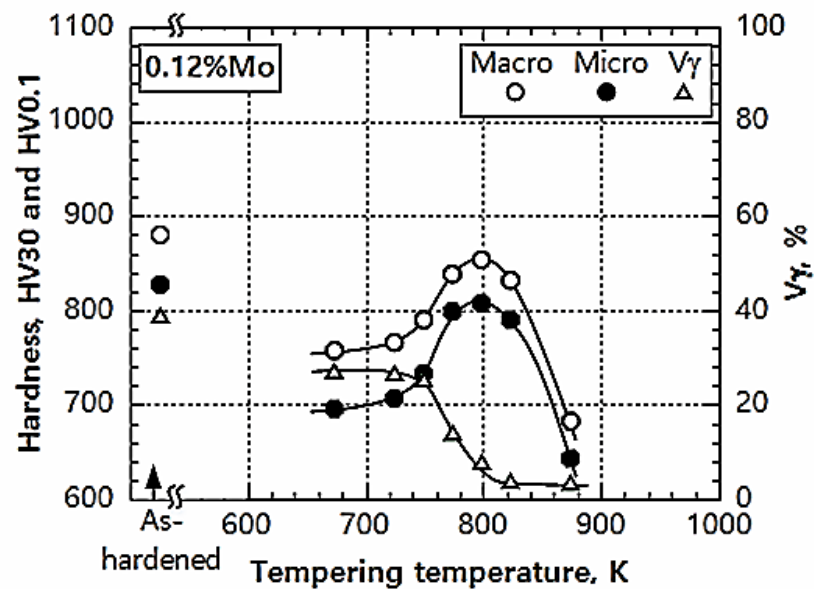
5.3.2 Effect of tempering temperature on hardness and volume fraction of retained austenite (Vγ)

After hardening, the specimens were tempered at several temperatures. The effect of tempering temperature on the macro- and micro-hardness and Vγ of each specimen is respectively shown in Fig. 5-9 (a) – (e). The macro-hardness shows similar behavior to the micro-hardness of all the specimens; that is, both of the hardness drops sharply from as-hardened state and then increases gradually to them maximum hardness as the tempering temperature increases. The H_{Tmax} of macro- and micro-hardness are obtained at same temperature, where the matrix structure is composed of martensite, secondary carbides with some retained austenite. In the tempering over the temperature at which H_{Tmax} is obtained, the hardness continues to decrease greatly due to the cohesion of secondary carbides and the transformation of austenite to ferrite.

When the specimen tempered at the lowest temperature of 673K, the hardness drops largely from that in as-hardened state because the martensite is tempered. However, the precipitation of fine secondary carbides takes place. As the tempering temperature is evaluated, the depletion of alloying element in austenite occurs by the precipitation of secondary carbides and it raises the Ms temperature. Resultantly, more martensite is produced since this phenomenon continues to around 773K where the carbide reaction starts, the hardness also continues to rise. Here, the carbide reaction in the tempering is displayed by the schematic flow chart in Fig. 5-10.

In the tempering at over 773K, the carbide reaction explained in Fig. 5-10 is already occurring, i.e. each alloying element forms every pure carbide like VC, Mo_2C, and W_2C. Because they have much higher hardness compared with those of M-type carbides, the total hardness increases more to reach the H_{Tmax} obtained by 798K

tempering.   When the tempering temperature gets over 798K, however, the agglomeration of their pure carbides takes due to the Ostwald ripening effect. This reaction makes the hardness drop remarkably.

(a) Specimen No. 1 (0.12%Mo)
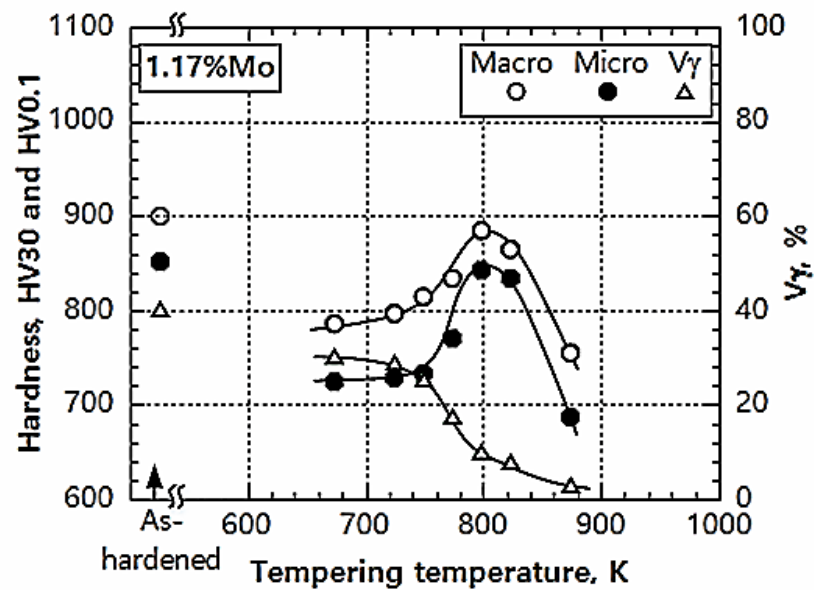
(b) Specimen No. 2 (1.17%Mo)
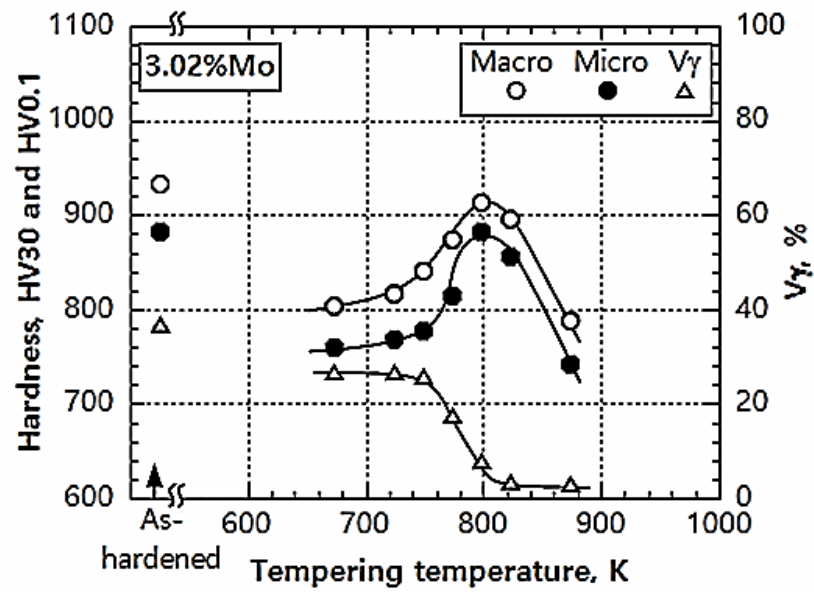
(c) Specimen No 3 (3.02%Mo)
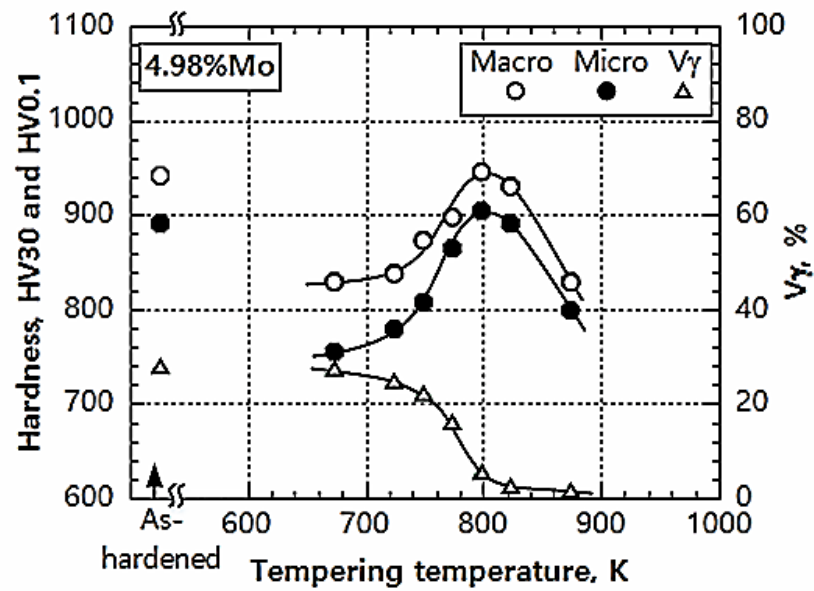
(d) Specimen No. 4 (4.98%Mo)
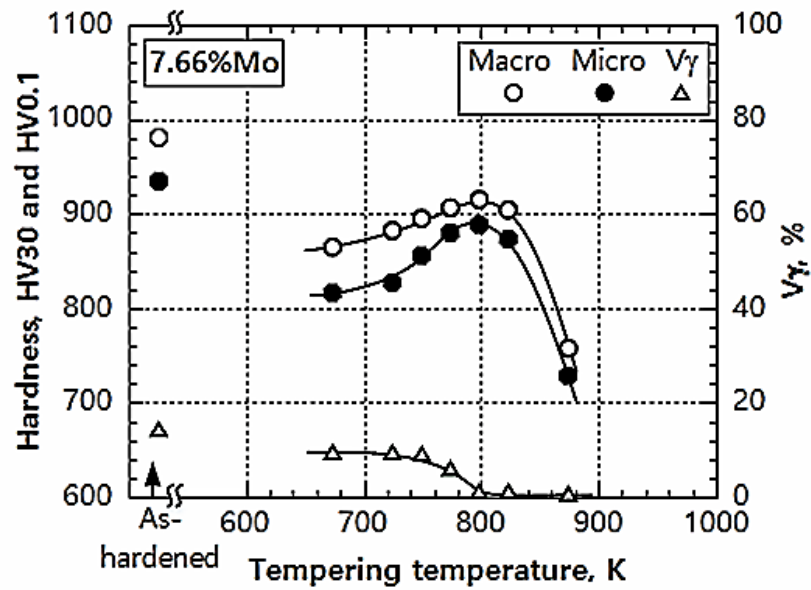
(e) Specimen No. 5 (7.66%Mo)

Fig. 5-9 Effect of tempering temperature on macro- and micro-hardness and volume fraction of retained austenite (Vγ). (a) 0.12% Mo, (b) 1.17% Mo, (c) 3.02%Mo, (d) 4.98%Mo and (e) 7.66%Mo specimens.
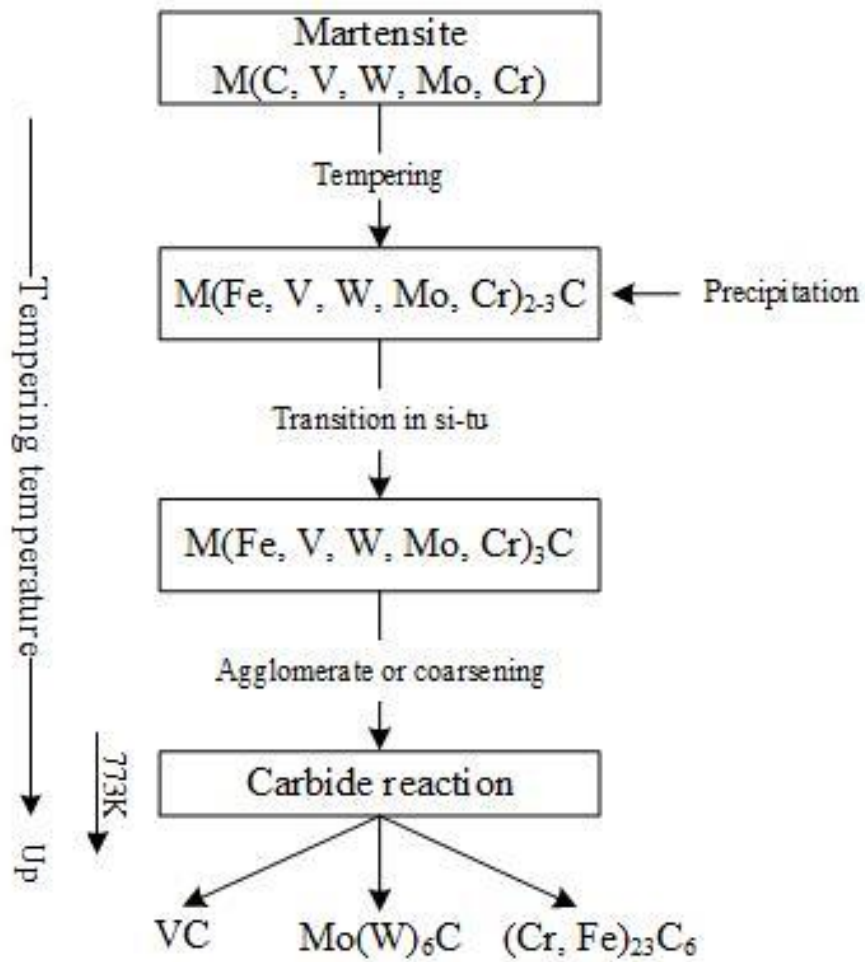
Note: Pure carbide with extremely high hardness forms by order of carbide forming ability.

Fig. 5-10 Schematic flow chart explaining tempering mechanism from martensite and carbide reaction in si-tu of multi-alloyed white cast iron.

As described in previous section, the tempering curves of macro- and micro- hardness showed similar trend. The macro- hardness is overall higher than the micro- hardness in all the specimens because the macro- hardness is the sum of hardness of eutectic carbides and the matrix. The differences between the macro- and micro- hardness at the H_{Tmax} are 47 HV in 0.12%Mo, 43 HV in 1.17%Mo, 29 HV in 3.02%Mo, 41 HV in 4.98% Mo and 27 HV in 7.66%Mo specimens, respectively.

A reduction of $V\gamma$ in matrix contributes to the increase of hardness reasonably. As the tempering temperature is increased, the $V\gamma$ began to decrease markedly over 748K. This means that the transformation rate of austenite to martensite is high in the range of 748 - 823K. It can be understood that an increases in a number of precipitated carbides reduces stability of retained austenite and encourages for austenite to transform into martensite. Conversely, the temperature rises to the over- tempering region over 823K, austenite transforms to pearlite or ferrite and therefore, the $V\gamma$ decreases close to nil.

5.3.3 Relation of hardness and retained austenite in tempered state

As mention before, the hardness and Vγ vary depending on the tempering temperature and Mo content. The morphology of eutectic carbide changes little during tempering because of low temperature. Therefore, the hardness in tempered state is influenced mainly by the constituent phases in matrix.

The relationships between macro- and micro-hardness and Vγ of all tempered specimens are presented in Fig. 5-11 (a) and (b). Though the data are scattered in a range, the macro- and micro-hardness show similar behavior and they increase to the maximum value and then decreases as the Vγ increases. The distribution of macro-hardness is located at higher hardness position and some specimens with macro-hardness more than 900 HV30 is obtained at about 2 to 16% Vγ. As for the micro-hardness, the distribution and scattering are similar to the case of micro-hardness. The maximum values of 940 HV30 for macro-hardness and 905 HV0.1 for micro-hardness are obtained at the Vγ of 5% and so. Such maximum values are mostly obtained in the test piece with 4.98% Mo. The specimens with low hardness at low Vγ are due to the over-tempering. On the other hand, the decrease in hardness over the maximum hardness is due to a rise of Vγ value.
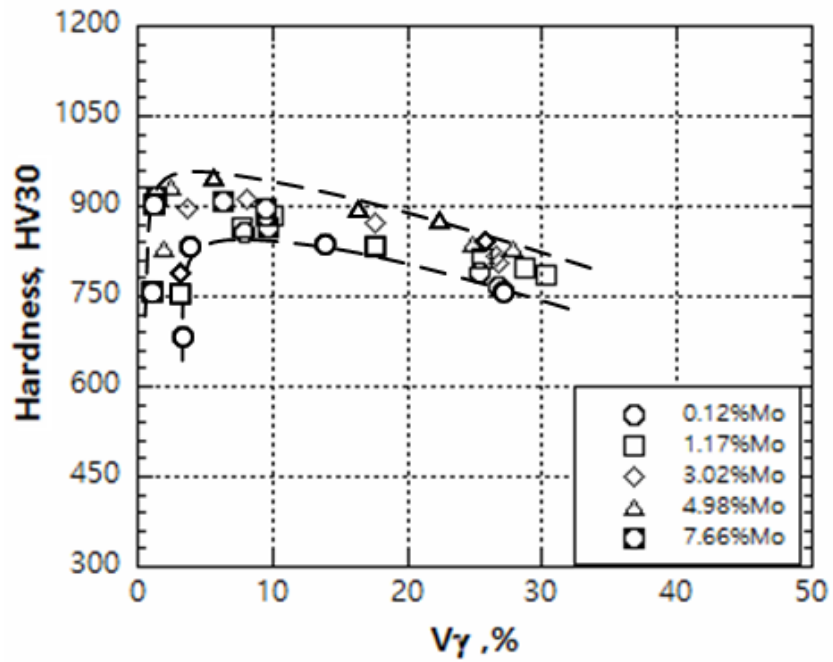
(a) Macro-hardness
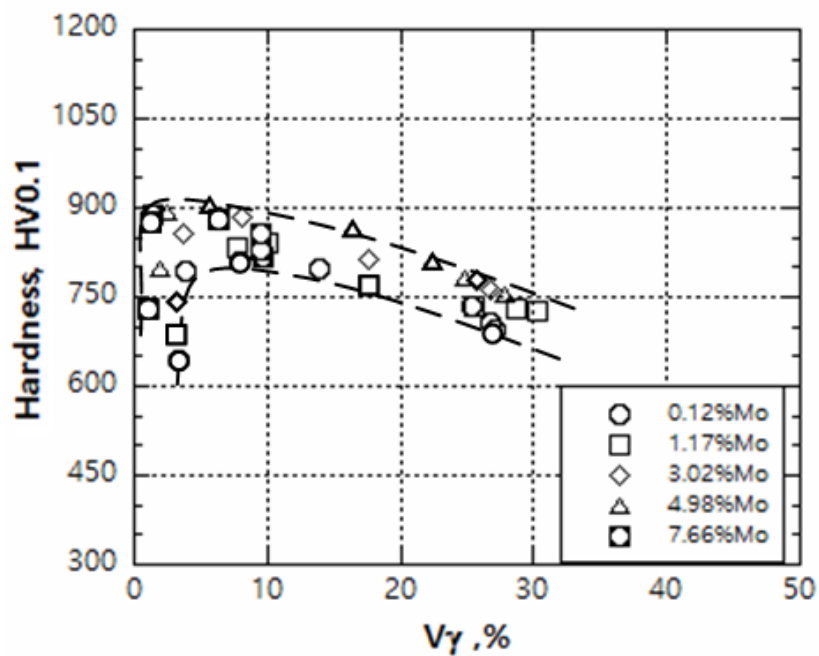
(b) Micro-hardness

Fig. 5-11 Relationship between macro- and micro-hardness and volume fraction of

retained austenite ($V\gamma$) of tempered specimens.

5.3.4 Effect of Mo on the maximum tempered hardness (H$_{Tmax}$)

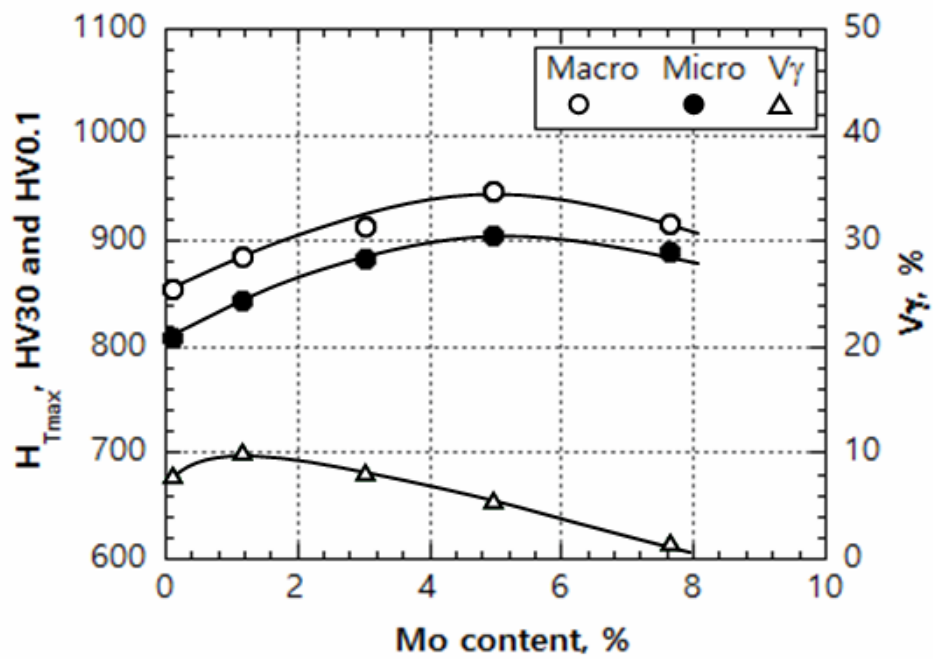The effect of Mo content on the H$_{Tmax}$ and Vγ at H$_{Tmax}$ is shown in Fig. 5.12. The H$_{Tmax}$ values of macro- and micro-hardness show similar variation corresponding with Mo content of the specimen. Both of hardness increase to the highest value at 4.98%Mo and then, decrease a little as Mo content increases. The Vγ value at the H$_{Tmax}$ is a little increased at 1.17%Mo and then, continues to decrease proportionally as the Mo content rises. It is found that the Vγ value at H$_{Tmax}$ of each specimen is overall less than 10%. This suggests that even if the test piece shows the maximum hardness in tempering, a certain amount of austenite remains.

From above results, it is believed that the Mo content of the cast iron affects the maximum hardness significantly. To explain the variation of the H$_{Tmax}$, the SEM observation of specimens with H$_{Tmax}$ are carried out focusing on the matrix in the specimen and their microphotographs are shown in Fig. 5-13 (a) – (e). The matrix microstructures of all specimens consist of secondary carbide (Sc), martensite (M) and retained austenite (γ_R). The size and amount of secondary carbides, as well as the amount of retained austenite, are different by increasing the Mo content. The fine secondary carbides are observed in 0.12 - 4.98%Mo specimens but coarse secondary carbides are found in 7.66%Mo specimen. It seems that the secondary carbides are increased in number as Mo content increases except for 7.66%Mo specimen. Even if the precipitated secondary carbides are mainly MC or M$_6$C types [27], the M$_2$C carbide could precipitate secondarily as same as the specimens with high Mo content such as 4.98% and 7.66%Mo. Since the special carbides have extremely high hardness, those carbides promote the secondary hardening greatly. In the case of 7.66%Mo specimen, however, the large massed carbides produced by

cohering of fine carbide increases in number and they lowers the matrix hardness. A decrease in hardness of martensite which is caused by the reduction of C in austenite can be another reason.

Fig. 5-12 Effect of Mo content on maximum tempered hardness (H_{Tmax}) and volume fraction of retained austenite ($V\gamma$) at H_{Tmax}.
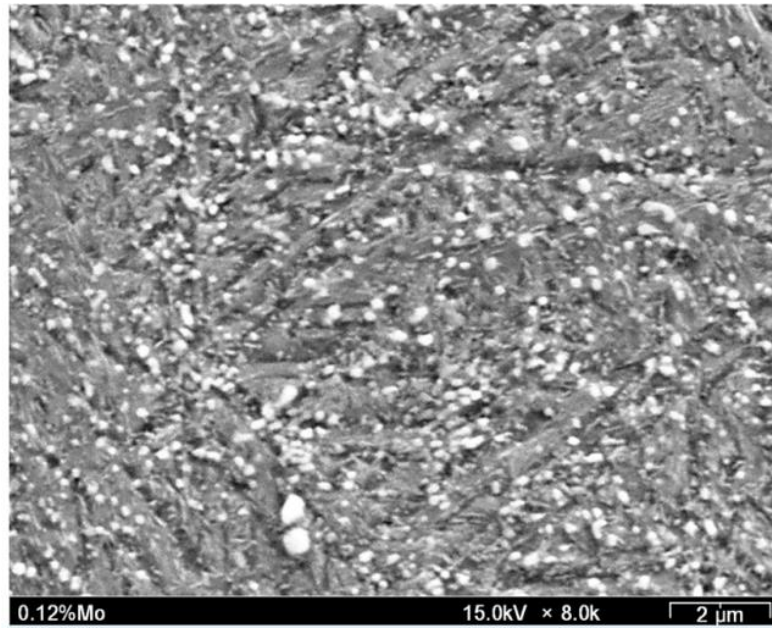
(a) Specimen No 1 **(**0.12**%**Mo**)**
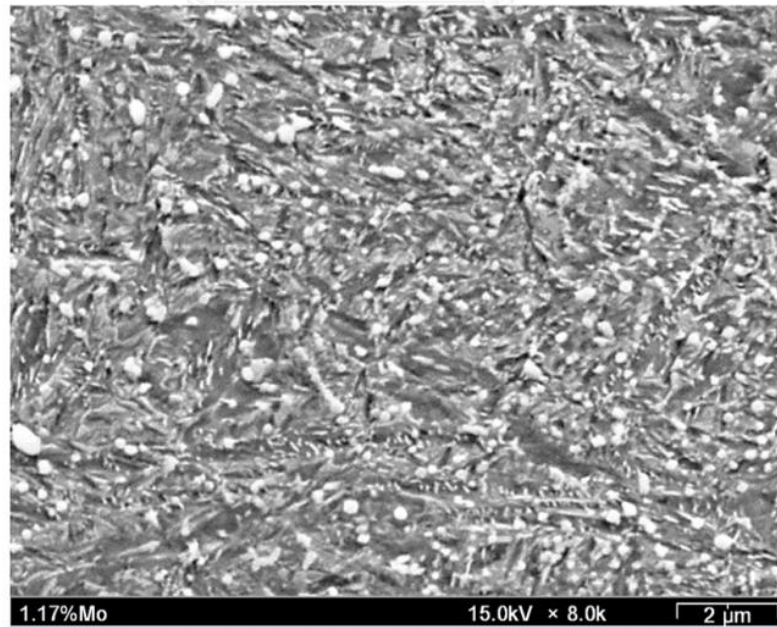
(b) Specimen No 2 **(**1.17**%**Mo**)**
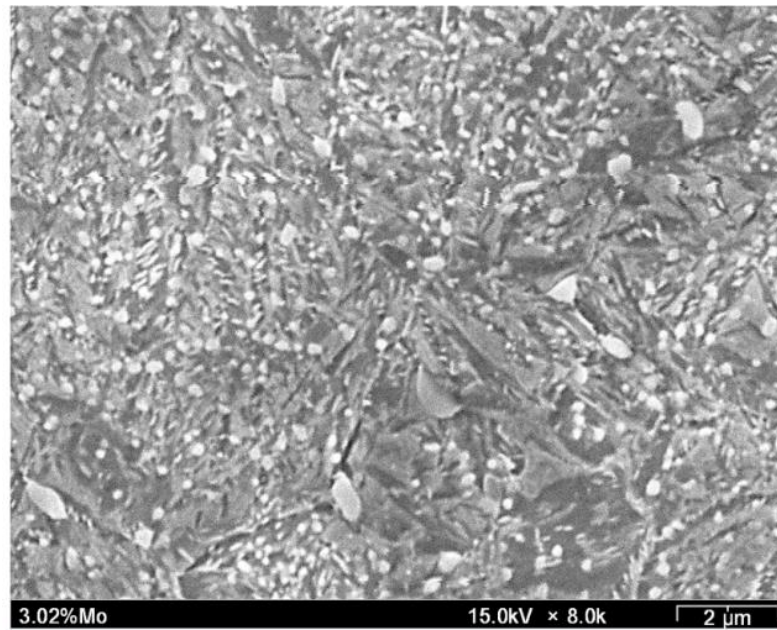
(c) Specimen No. 3 **(**3.02**%**Mo**)**
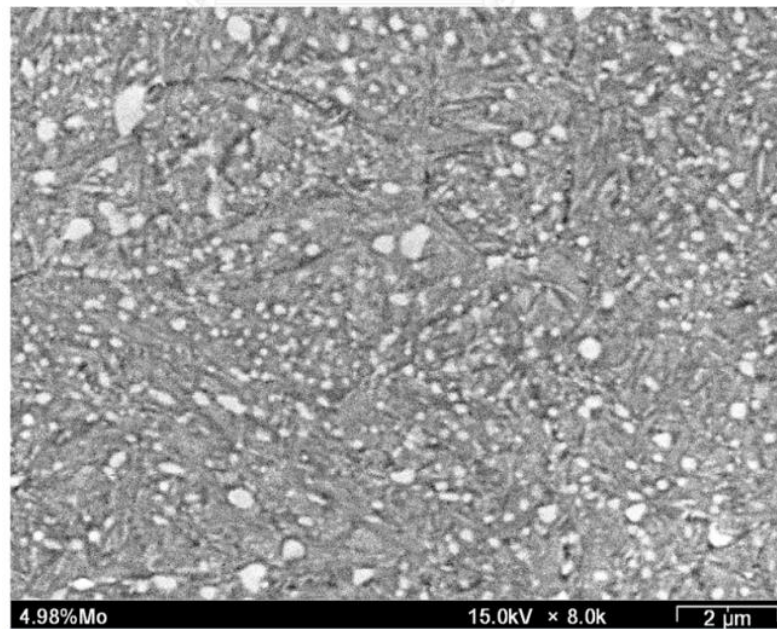
(d) Specimen No. 4 **(**4.98**%**Mo**)**
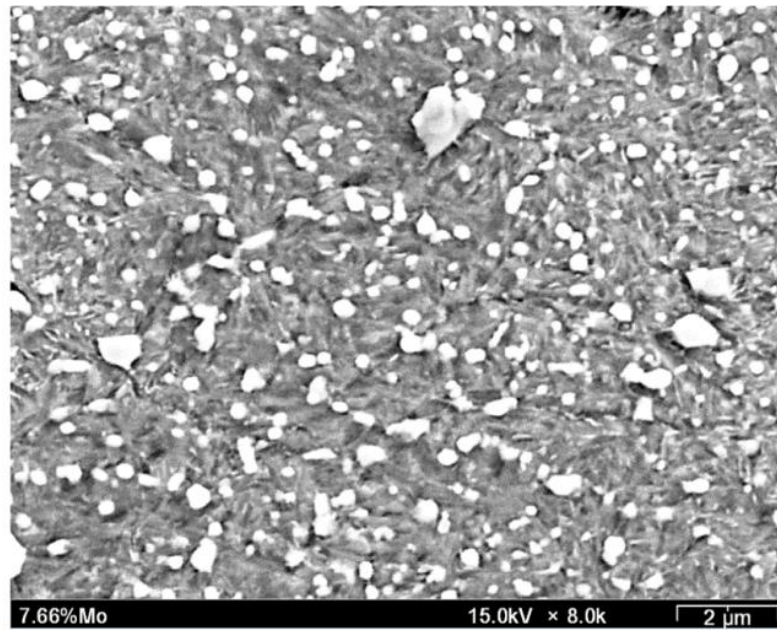
(e) Specimen No 5 (7.66%Mo)

Fig. 5-13 SEM microphotographs of specimen with H_{Tmax}. (a) 0.12%Mo, (b) 1.17%Mo,

(c) 3.02%Mo, (d) 4.98%Mo and (e) 7.66%Mo specimens.

As discussed previously, the variation of hardness is mainly affected by the type and amount of precipitated carbides in matrix. Therefore, the identification of secondary carbides was tried by EDS analyzes. In each tempered specimen, fifteen carbide particles were picked up and quantitative analysis of four alloying elements, Cr, Mo, W and V, were carried out. The results are summarized in Table 5-1. Since it was impossible to obtain the absolute values of alloy concentration because the size of carbides are too small for the X-ray beam to irradiate within area of carbide particle. However, it can be found which carbide shows the highest value of element. It can be presumed from Table 5-1 what kinds of carbides are existing in the matrix of specimen. In the specimen No. 1 with 0.12%Mo to No. 3 with 3.02%Mo, VC as V-rich and $Cr_{23}C_6$ as Cr-rich carbides precipitated. In specimen No. 4 with 4.98% Mo, M_6C as (Mo, W)-rich carbide precipitated additionally, and so three kinds of special carbides existed in the matrix. In the matrix of specimen No. 5 with highest Mo content of 7.66%Mo, however, the secondary carbides were all M_6C carbides. From there results it can be understood that the specimen No. 4 showed the highest value of H_{Tmax} due to the precipitation of many M_2C special carbides with very high hardness.

Table 5-1 Estimation of the type of secondary carbide precipitated in tempered matrix.

| Specimen	Type of secondary carbide		
	V-rich	(Mo, W)-rich	Cr-rich
No. 1 (0.12%Mo)	3		12
No. 2 (1.17%Mo)	5		10
No. 3 (3.02%Mo)	3		12
No. 4 (4.98%Mo)	1	6	8
No. 5 (7.66%Mo)		15	

5.3.5 Effect of volume fraction of retained austenite (V_γ) in as-hardened state on maximum tempered hardness (H_{Tmax}).

In order to clarify how the $V\gamma$ in as-hardened state effect on the hardness in tempered state, the H_{Tmax} values are connected to the V_γ in as-hardened state and the relationship is shown in Fig. 5-16. In the relation, the high values of H_{Tmax} are obtained in the region from 15 to 28% V_γ. The H_{Tmax} decreases over 30% V_γ in as-hardened state because the excessive retained austenite remains after tempering and it reduces the matrix hardness more than the secondary hardening by the precipitation of carbides and the transformation of martensite. It is clearly from the fact that 15-30% $V\gamma$ in the as-hardened state is necessary to obtain the high H_{Tmax} values over about 900 HV30 by tempering. This demonstrates that the $V\gamma$ in as-hardened state contribute more to the secondary hardening, that is, the precipitation of special carbides and the transformation of austenite to martensite during tempering.
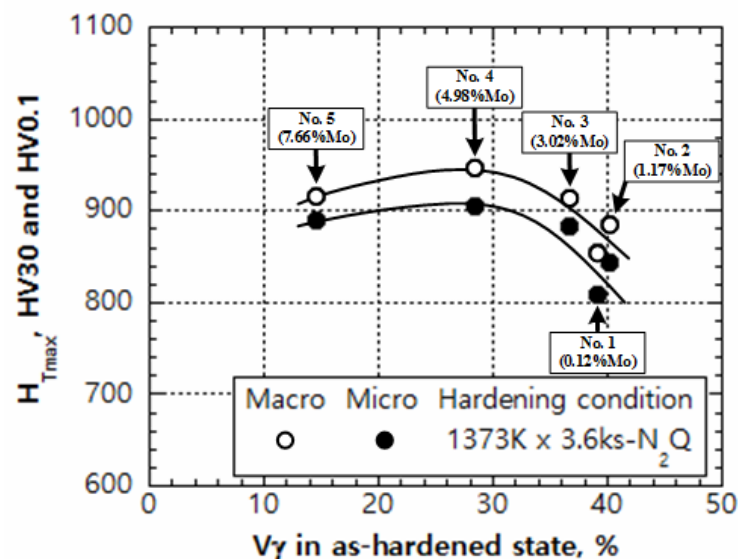
Fig. 5-14 Relationship between maximum tempered hardness (H_{Tmax}) and volume fraction of retained austenite ($V\gamma$) in as-hardened state.

5.3.6 Effect of Mo content on degree of secondary hardening (ΔHs)

As shown in Fig. 5-9, the tempered hardness curve of each specimen displays the secondary hardening evidently. It is considered that the Mo content as well as the V_γ in as-hardened state should affect the degree of secondary hardening (ΔHs) of which definition was described in section 4.2.2.1. Relationship between ΔHs and Mo content is shown in Fig. 5-15. As the Mo content rises, the ΔHs increases to the largest ΔHs at 4.98% Mo. After that, the ΔHs is lowered remarkably toward 7.66% Mo. It is noted that the ΔHs of micro-hardness is overall higher than that of macro-hardness. The largest ΔHs for micro-hardness is 150 HV0.1 and it is obtained at 4.98% Mo.

From these findings, it can be said that the secondary hardening is accomplished due to the change in matrix structure which is determined by precipitation of secondary carbides including the formation of pure carbide occurred in the carbide reaction. The transformation of martensite from the rest of austenite is an additional reason. In addition, it is considered that the transformations mentioned just before are mainly influenced by the $V\gamma$ value in as-hardened state. Therefore, the difference between $V\gamma$ in as-hardened state and $V\gamma$ at H_{Tmax} (Δ$V\gamma$), which means the amount of reduced austenite during tempering, were related to the ΔHs.

Relation of the ΔHs vs. Δ$V\gamma$ is shown in Fig. 5-16. The highest ΔHs is obtained at 22%Δ$V\gamma$. In the region of Δ$V\gamma$ less than 22%, the ΔHs is reduced greatly as the Δ$V\gamma$ decreased. Even if the Δ$V\gamma$ rises to around 30%, the ΔHs does not decrease so much and keeps the ΔHs over 100 HV0.1. This suggests that relatively large amount of Δ$V\gamma$ is necessary to get a large degree of secondary hardening. Since the $V\gamma$ in as-hardened state is determined by the amount of Mo dissolved in austenite matrix, the ΔHs is

indirectly influenced by the Mo content of the specimen. So, it can be explained that Mo promotes the secondary hardening by precipitating more special Mo carbide with high hardness.
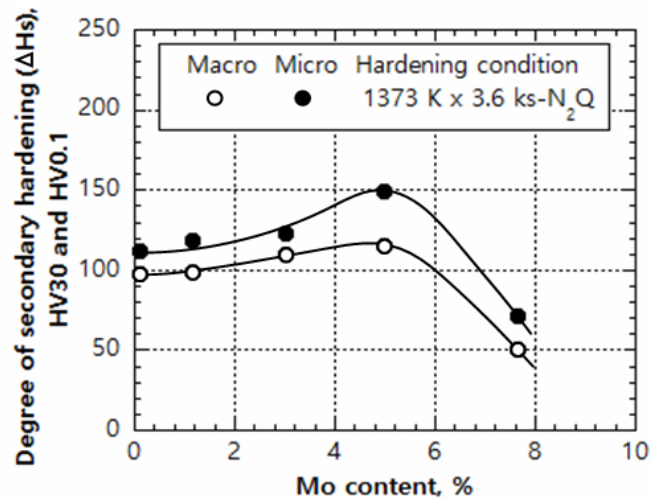
Fig. 5-15 Relationship between degree of secondary hardening (ΔHs) and Mo content.
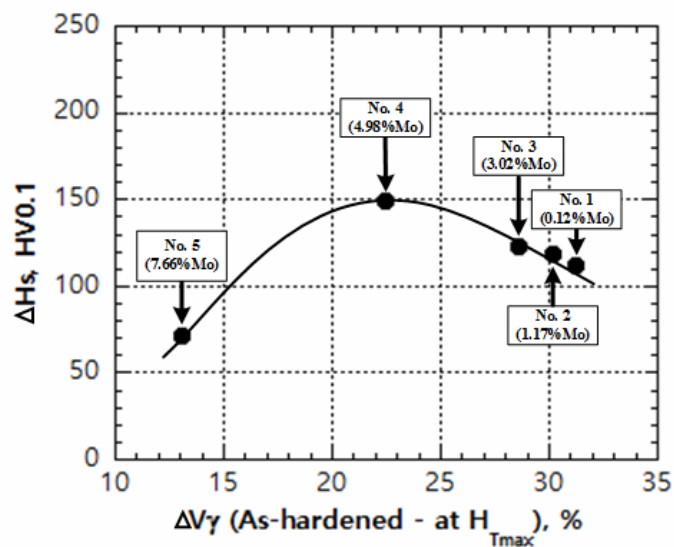
Fig. 5- 16 Relationship between difference of $V\gamma$ in as- hardened state and $V\gamma$ at H_{Tmax} ($\Delta V\gamma$) and degree of secondary hardening (ΔHs).

Chapter VI
Conclusions

The Mo content was varied widely from 0.12% to 7.66% Mo in multi-allayed white cast irons with basic composition, and the effect of Mo content on heat treatment behavior was investigated. First of all, the as-cast microstructures of test specimens were verified by the thermal analysis technique. The as-cast specimens were annealed at 1223K for 18 ks. After annealing, the test pieces in disk shape were austenitized at 1,373K for 3.6 ks in a vacuum furnace and then hardened by quenching with jet-spray of liquid nitrogen. The tempering was done at the temperatures between 673 K to 873 K by 50 K interval for 12 ks. The microstructure was observed by optical microscope (OM) and scanning electron microscope (SEM). The hardness was measured by the Vicker's hardness tester and volume fraction of retained austenite ($V\gamma$) was calculated by the method of X-ray diffraction method (XRD).

6.1 Effect of Mo content on microstructure and heat treatment behavior

6.1.1 Microstructure of as-cast specimens

1) All the as-cast specimens show hypo eutectic structure which consists of austenite dendrite and eutectic structures. The eutectic structures of (γ+MC) and (γ+M_7C_3) types were observed in the 0.12 and 1.17%Mo specimens and (γ+MC) and (γ+M_2C) eutectics were found in 3.02%, 4.98% and 7.66% Mo specimens.

2) According to thermal analysis curve, solidification of specimens with Mo content more than 3% begin with primary austenite (γ_p), followed by the eutectic reactions of L $\rightarrow$ (γ+MC)$_E$ and then, L $\rightarrow$ (γ+M_2C)$_E$, respectively. The solidification

temperature range of (γ+MC) eutectic decreases but that of (γ+M$_2$C) eutectic increases with an increase in Mo content.

3) The area fraction of primary austenite (γ_p) and the total amount of eutectic structures were almost constant of 47% and 53%, respectively, regardless of Mo content. However, the area fraction of (γ+MC) eutectic is decreased while (γ+M$_2$C) eutectic is increased with an increase in Mo content.

4) As Mo content increases, the start to solidify temperature of (γ+M$_2$C) eutectic increases.

6.1.2 Microstructure of as-hardened specimens

The matrix of all the specimens was composed of precipitated secondary carbide, martensite and retained austenite (γ_R). It seems that the amount of secondary carbide and martensite increased as well as the retained austenite decreased with increasing the Mo content.

6.1.3 Microstructure of tempered specimens

1) The matrix structure of tempered specimen was consisted of secondary carbides much more than those in as-hardened state and martensite together with retained austenite (γ_R) except for the specimens tempered over 798K in which coarser secondary carbides and ferrite existed. The amount of carbide was increased by elevating tempering temperature but on the contrary, the amount of retained austenite was lowered.

2) Analyzing alloy concentrations of the secondary carbides in matrix, the type of secondary carbide could be classified to V-rich, (Mo, W)-rich and Cr-rich carbides.

In the specimen No. 1 with 0.12%Mo to No. 3 with 3.02%Mo could found only V-rich and Cr-rich carbides. The (Mo, W)-rich carbide was found in the specimen with 4.98%Mo together with Cr-rich and V-rich carbides. In the specimen with 7.66%Mo, only Mo-rich carbide existed.

6.2 Effect of Mo content on macro-and micro- hardness and volume fraction of retained austenite (V_γ)

6.2.1 As-cast state

1) The macro-hardness which is measured as the sum of hardness of eutectics and matrices together, while micro-hardness is measured in only matrix including secondary carbides and other phases. Therefore, the macro-hardness always shows higher value than micro-hardness.

2) Both of Macro- and micro-hardness are increased to the maximum value at 3.02%Mo and then decreased with an increase in Mo content.

3) The volume fraction of retained austenite (V_γ) showed similar trend to the hardness, and it is increased continuously as Mo content increases to 3.02%Mo. As Mo content increases more over 3.02%Mo, the V_γ decreases because more Mo and C are consumed to form the ($\gamma+M_2C$) eutectic during solidification. As a result of decreasing the Mo and C contents in matrix, the V_γ decreases.

6.2.2 As-hardened state

1) The macro- and micro-hardness are increased progressively with an increase in Mo content because the amount of secondary carbide rises. The highest macro- and micro-hardness are obtained in the specimen with highest Mo content of 7.66%.

2) The volume fraction of retained austenite ($V\gamma$) decreases markedly when Mo content is raised over 1.17%Mo.

6.2.3 Tempered state

1) The tempered hardness curve shows an evident secondary hardening at which lots of fine secondary carbides precipitate and the volume fraction of retained austenite ($V\gamma$) is low. Especially, the carbide reaction from martensite formed by hardening takes place actively, and martensite transformation from the rest of austenite also occurs.

2) The $V\gamma$ value in each specimen trends to decrease as the tempering temperature increases and greatly in the tempering at 748 - 823K.

3) The tempered hardness with more than 900 HV30 is obtained in specimens which have the $V\gamma$ value of 2 to 18% that corresponds to the specimens with 3.02% to 7.66%Mo.

4) The 15-35% $V\gamma$ in the as-hardened state is necessary to get the hardness over 900 HV30.

6.2.4 Relationship between maximum tempered hardness (H_{Tmax}) and volume fraction of retained austenite ($V\gamma$) in heat-treated state

1) The maximum tempered hardness (H_{Tmax}) was obtained at 798K tempering in all of specimens.

2) The H_{Tmax} increased first and thereafter, decreased with an increase in Mo content. The highest H_{Tmax} value of 946 HV30 and 906 HV0.1 are obtained in the specimens with 4.98%Mo and 5.56%V_γ.

3) The $V\gamma$ values at H_{Tmax} of all the specimens are less than 10%, and the highest H_{Tmax} value is obtained at 5.6%V_γ.

4) The degree of secondary hardening (ΔHs) increases as Mo content rises from nil to 4.98% where the difference of $V\gamma$ between $V\gamma$ in as-hardened state and that at H_{Tmax} ($\Delta V\gamma$) is 22.5%.

REFERENCES

1.   Hashimoto, M., *Development of multi-component white cast iron rolls and rolling technology in steel rolling.* Proceedings of ABRASION 2008, 2008: p. 1-23.

2.   Boccalini Jr, M., A. Sinatora, and Y. Matsubara. *Overview: high speed steels for hot rolling mill rolls.* in *Proceedings.* 2000.

3.   Kang, Y., et al., *Effects of carbon and chromium additions on the wear resistance and surface roughness of cast high-speed steel rolls.* Metallurgical and Materials Transactions A, 2001. **32**(10): p. 2515-2525.

4.   Kim, C., et al., *Effects of alloying elements on microstructure, hardness, and fracture toughness of centrifugally cast high-speed steel rolls.* Metallurgical and Materials Transactions A, 2005. **36**(1): p. 87-97.

5.   Matsubara, Y. *Development and applications of Multi-alloyed white cast iron for rolling and pulverizing mills.* in *The fifth International Conference on Science, Techonology and Innovation for Sustainable Well-Being.* 2013. Laos PDR.

6.   Thisen, W. and G. Gevelmuann. *New wear resistance cast alloys for use at elevated temperature.* in *Abrasion 2011.* 2011. Belgium.

7.   HASHIMOTO, et al., *Analysis of carbides in multi-component white cast iron for hot rolling mill rolls.* Vol. 44. 2004, Tokyo, JAPON: Iron and Steel Institute of Japan. 9.

8.   Fu, H., Q. Xiao, and J. Xing, *A study of segregation mechanism in centrifugal cast high speed steel rolls.* Materials Science and Engineering: A, 2008. **479**(1–2): p. 253-260.

9.   Sasaguri, N., et al., *Influence of cobalt content on heat treatment behaivoir and abrasive wear characterisitics of multi-component white cast iron.* J. JFS, 2010. **82**(11): p. 667-673.

10.   Luan, Y., et al., *Effect of solidification rate on the morphology and distribution of eutectic carbides in centrifugal casting high-speed steel rolls.* Journal of Materials Processing Technology, 2010. **210**(3): p. 536-541.

11.   Fu, H., Q. Xiao, and Y. Li, *A study of the microstructures and properties of Fe–V–W–Mo alloy modified by rare earth.* Materials Science and Engineering: A, 2005. **395**(1–2): p. 281-287.

12.   Inthidech, S., P. Sricharoenchai, and Y. Matsubara, *Effect of alloying elements on heat treatment behavior of hypoeutectic high chromium cast iron.* Materials transactions, 2006. **47**(1): p. 72-81.

13.   Materials, T.J.I.o.M.a., *Kingoku Data Book* 1974, Japan.

14.   HASHIMOTO, *Effect of alloying element on compressive and wear properties of multi-component white cast iron for steel rolling mill rolls*, in *Abrasion 2011*. 2011: Belgium. p. 183-192.

15.   Matsubara, Y., et al., *Solidification and abrasion wear of white cast irons alloyed with 20% carbide forming elements.* Wear, 2001. **250**(1–12): p. 502-510.

16.   Molinari, A., et al. *Primary carbides in spincast HSS for hot rolls and their effect on the oxidation behaviour*. in *Proceedings of the 6th Tooling Conference, Sweden*. 2002.

17.   Hwang, K.C., S. Lee, and H.C. Lee, *Effects of alloying elements on microstructure and fracture properties of cast high speed steel rolls: Part I:*

Microstructural analysis. Materials Science and Engineering: A, 1998. **254**(1–2): p. 282-295.

18.   BOCCALINI JR, M., et al. *Effects of vanadium content and cooling rate on the solidification of multi-component white cast iron.* in *INTERNATIONAL CONFERENCE OF THE SCIENCE OF CASTING AND SOLIDIFICATION.* 2001.

19.   Scandian, C., et al., *Effect of molybdenum and chromium contents in sliding wear of high-chromium white cast iron: The relationship between microstructure and wear.* Wear, 2009. **267**(1–4): p. 401-408.

20.   Junhua, K., et al., *Influence of Mo content on microstructure and mechanical properties of high strength pipeline steel.* Materials & Design, 2004. **25**(8): p. 723-728.

21.   Wu, H.-Q., et al., *Solidification of multi-alloyed white cast iron: type and morphology of carbides.* Transactions of the American Foundrymen's Society, 1996. **104**: p. 103-108.

22.   Da Silva, C. and M. Boccalini, *Thermal cracking of multicomponent white cast iron.* Materials science and technology, 2005. **21**(5): p. 565-573.

23.   Lee, E.-S., et al., *Solidification microstructure and M2C carbide decomposition in a spray-formed high-speed steel.* Metallurgical and Materials Transactions A, 1998. **29**(5): p. 1395-1404.

24.   Theisen, W., *Design of wear resistant alloys against abrasion*, in *Abrasion 2008.* 2008: Italy.

25.   Imurai, S., et al., *Effects of Mo on microstructure of as-cast 28wt.% Cr–2.6wt.% C–(0–10) wt.% Mo irons.* Materials Characterization, 2014. **90**(0): p. 99-112.
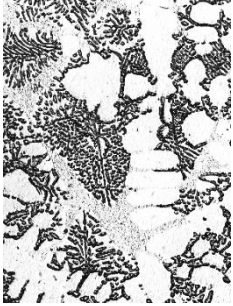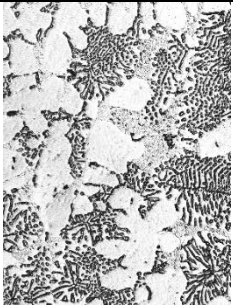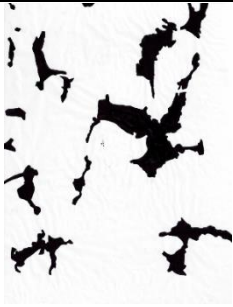
26.   Gasan, H. and F. Erturk, *Effects of a Destabilization Heat Treatment on the Microstructure and Abrasive Wear Beh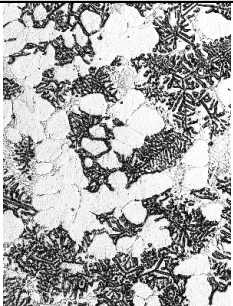avior of High-Chromium White Cast Iron Investigated Using Different Characterization Techniques.* Metallurgical and Materials Transactions A, 2013. **44**(11): p. 4993-5005.

27.   Khaninantharak, W., et al., *Effect of Carbon and Heat Treatment on the Hardness and Austenite Content of Multi-Component White Cast Iron.* AFS Transactions 2009, 2009: p. 09-018.

28.   Opapaiboon, J., et al., *Effect of Carbon Content on Heat Treatment Behavior of Multi-Alloyed White Cast Iron for Abrasive Wear Resistance.* Materials transactions, 2015(0).

29.   Wu, H.-Q., *Studies on Solidification Structure of Multi-Component White Cast Iron.* 2000, University of Tokyo japan. p. 178.
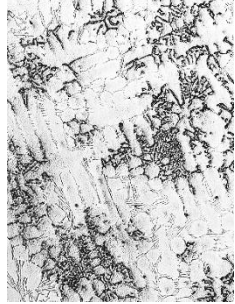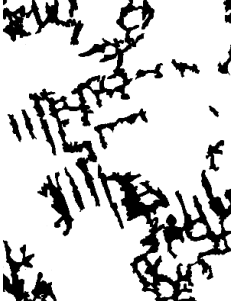
APPENDIX

Table 1 Example of tracing outline of each phase from microphotograph for area fraction measurement.

Specimen No. 1 (0.12%Mo)			
OM microstructure	Primary austenite	γ + MC	γ + M_7C_3
Specimen No. 2 (1.17%Mo)			
OM microstructure	Primary austenite	γ + MC	γ + M_7C_3
Specimen No. 3 (3.02%Mo)			
OM microstructure	Primary austenite	γ + MC	γ + M_2C

Specimen No. 4 (4.98%Mo)			
OM microstructure	Primary austenite	γ + MC	γ + M$_2$C

Specimen No. 5 (7.66%Mo)			
OM microstructure	Primary austenite	γ + MC	γ + M$_2$C

The variation of matrix microstructure in heat-treatment

(a) Specimen No. 1 (0.12%Mo)

As-hardened state	tempered at 723K for 12 ks
tempered at 773K for 12 ks	tempered at 798K for 12 ks
tempered at 823K for 12 ks	tempered at 873K for 12 ks

(b) Specimen No. 2 (1.17%Mo)

As-hardened state	tempered at 723K for 12 ks
tempered at 773K for 12 ks	tempered at 798K for 12 ks
tempered at 823K for 12 ks	tempered at 873K for 12 ks

(c) Specimen No.3 (3.02%Mo)

As-hardened state	tempered at 723K for 12 ks
tempered at 773K for 12 ks	tempered at 798K for 12 ks
tempered at 823K for 12 ks	tempered at 873K for 12 ks

(d) Specimen No.4 (4.98%Mo)

As-hardened state	tempered at 723K for 12 ks
tempered at 773K for 12 ks	tempered at 798K for 12 ks
tempered at 823K for 12 ks	tempered at 873K for 12 ks

(e) Specimen No. 5 (7.66%Mo)

As-hardened state	tempered at 723K for 12 ks
tempered at 773K for 12 ks	tempered at 798K for 12 ks
tempered at 823K for 12 ks	tempered at 873K for 12 ks

Table 2 Macro- and micro-hardness and volume fraction of retained austenite (V_γ) of specimens

| Specimen | Tempering temperature (K) | Hardness | | Volume fraction of retained austenite (V_γ) (%) |
		Macro (HV30)	Micro (HV0.1)	
Specimen No. 1 (0.12%Mo)	As-cast	625	597	32.29
	As-hardened	882	829	39.09
	673	757	696	27.13
	723	767	708	26.74
	748	791	735	25.43
	773	838	799	14.00
	798	855	808	7.88
	823	833	729	3.96
	873	683	644	3.37
Specimen No. 2 (1.17%Mo)	As-cast	655	644	35.83
	As-hardened	902	853	40.24
	673	787	725	30.26
	723	797	729	28.78
	748	815	733	25.51
	773	835	771	17.60
	798	886	843	10.05
	823	865	834	7.84
	873	756	688	3.15

Specimen	Tempering temperature (K)	Hardness		Volume fraction of retained austenite (V_γ) (%)
		Macro (HV30)	Micro (HV0.1)	
Specimen No. 3 (3.02%Mo)	As-cast	740	718	43.84
	As-hardened	934	884	36.70
	673	804	761	26.73
	723	818	768	26.58
	748	842	778	25.77
	773	873	815	17.62
	798	913	884	8.13
	823	897	856	3.70
	873	788	743	3.17
Specimen No. 4 (4.98%Mo)	As-cast	685	658	34.71
	As-hardened	941	892	28.05
	673	830	756	27.78
	723	838	780	24.85
	748	875	810	22.34
	773	898	865	16.36
	798	946	905	5.56
	823	930	893	2.52
	873	830	799	1.96

Specimen	Tempering temperature (K)	Hardness		Volume fraction of retained austenite (V_γ) (%)
		Macro (HV30)	Micro (HV0.1)	
Specimen No. 5 (7.66%Mo)	As-cast	643	617	23.06
	As-hardened	982	935	14.56
	673	866	818	9.65
	723	883	828	9.55
	748	896	856	9.44
	773	907	880	6.38
	798	916	889	1.50
	823	906	875	1.29
	873	758	729	1.09

Table 3 Degree of secondary hardening (ΔHs), The differences of V_γ in as-hardened state and H_{Tmax} (ΔV_γ) and ΔV_γ ration.

Specimen	Degree of secondary hardening (ΔHs)		The differences of V_γ in as-hardened state and H_{Tmax} (ΔV_γ) (%)	ΔV_γ ratio (%)
	Macro (HV30)	Micro (HV0.1)		
Specimen No. 1 (0.12%Mo)	97.8	112.2	31.2	79.8
Specimen No. 2 (1.17%Mo)	98.6	118.4	30.2	75.0
Specimen No. 3 (3.02%Mo)	109.2	123.2	28.6	77.9
Specimen No. 4 (4.98%Mo)	115.4	148.8	22.5	80.2
Specimen No. 5 (7.66%Mo)	50.2	71.4	13.1	89.7

VITA

My name is Thanit Meebupha. I was born on September 30, 1989 in Suphanburi. I graduated Bachelor's degree of Engineering (Materials Engineering) from Kasetsart University (Bangken campus) in 2011. After graduate, I have been studying for master degree of Engineering in Metallurgical Engineering at Chulalongkorn University. I was a research student at department of Materials Science and Metallurgical Engineering, National Institute of Technology, Kurume College japan in august 2015 until December 2015.